Synthesis and biological evaluation of biotin-conjugated anticancer thiosemicarbazones and their iron(III) and copper(II) complexes

Sebastian Kallus[‡,⊥], Lukas Uhlik[#,⊥], Sushilla van Schoonhoven[#], Karla Pelivan[‡], Walter Berger[#,§], Éva A. Enyedy[†], Thilo Hofmann[$], Petra Heffeter[#,§,], Christian R. Kowol[‡,§,*], Bernhard K. Keppler[‡,§]*

[‡] Institute of Inorganic Chemistry, Faculty of Chemistry, University of Vienna, Waehringer Str. 42, A-1090 Vienna, Austria

[#] Institute of Cancer Research and Comprehensive Cancer Center, Medical University of Vienna, Borschkeg. 8a, A-1090 Vienna, Austria

[§] Research Cluster "Translational Cancer Therapy Research", Vienna, Austria

[†] Department of Inorganic and Analytical Chemistry, University of Szeged, Dóm tér 7, H-6720, Szeged, Hungary

[$] Department of Environmental Geosciences, University of Vienna, Althanstraße 14, A-1090, Vienna, Austria.

[⊥] These authors contributed equally to this work

Dedicated to Prof. Dr. Peter Comba on the occasion of his 65th birthday.

*__Authors for correspondence:__ Institute of Inorganic Chemistry, University of Vienna, Waehringer Str. 42, A-1090 Vienna, Austria. Phone: +43-1-4277-52609. Fax: +43-1-4277-52680. E-mail: christian.kowol@univie.ac.at

Institute of Cancer Research, Medical University of Vienna, Borschkeg. 8a, A-1090 Vienna, Austria. Phone: +43-1-40160-57557. Fax: +43-1-40160-957555. E-mail: petra.heffeter@meduniwien.ac.at

Conflicts of interest

The authors declare no conflicts of interest.

Key words: Thiosemicarbazones, Triapine, biotin targeting, metal complexes

Abstract

Triapine, the most prominent anticancer drug candidate from the substance class of thiosemicarbazones, was investigated in more than 30 clinical phase I and II studies. However, the results were rather disappointing against solid tumors, which can be explained (at least partially) due to inefficient delivery to the tumor site. Hence, we synthesized the first biotin-functionalized thiosemicarbazone derivatives in order to increase tumor specificity and accumulation. Additionally, for Triapine and one biotin conjugate the iron(III) and copper(II) complexes were prepared. Subsequently, the novel compounds were biologically evaluated on a cell line panel with different biotin uptake. The metal-free biotin-conjugated ligands showed comparable activity to the reference compound Triapine. However, astonishingly, the metal complexes of the biotinylated derivative showed strikingly decreased anticancer activity. To further analyze possible differences between the metal complexes, detailed physico- and electrochemical experiments were performed. However, neither lipophilicity or complex solution stability, nor the reduction potential or behavior in the presence of biologically relevant reducing agents showed strong variations between the biotinylated and non-biotinylated derivatives (only some variations in the reduction kinetics were found). Nonetheless, the metal-free biotin-conjugate of Triapine revealed distinct activity in a colon cancer mouse model upon oral application comparable to Triapine. Therefore, this type of biotin-conjugated thiosemicarbazone is of interest for further synthetic strategies and biological studies.

Introduction

Since several decades, α-*N*-heterocyclic thiosemicarbazones have been investigated for their potential as anticancer therapeutics[1, 2]. As biological target ribonucleotide reductase (RR) has been proposed, a metalloenzyme catalyzing the conversion of ribonucleotides to 2'-deoxyribonucleotides, making it essential for DNA synthesis and repair[3]. In fact, thiosemicarbazones are the strongest known inhibitors of this enzyme being several orders of magnitude more efficient than hydroxyurea, the first clinically approved RR inhibitor[4, 5]. While the exact mode of action of thiosemicarbazones is still unknown, they most likely bind intracellular iron *via* their *NNS*-donor atoms. It is assumed that the resulting iron complex interacts with the RR and as a consequence disturbs DNA synthesis. Moreover, complexation of other biologically relevant metals such as copper has been discussed to be important for the mode of action of (at least some) thiosemicarbazones, since their mono-ligand copper(II) complexes have proven exceptionally high stability[6, 7]. The clinically most prominent representative of the substance class of thiosemicarbazones is 3-aminopyridine-2-carboxaldehyde thiosemicarbazone (Triapine) which has already been evaluated in more than 30 clinical phase I and II studies[8-11]. While Triapine was activity against leukemia, there was no effect against solid cancers such as non-small-cell lung cancer[12] or renal cell carcinoma[13]. The exact reasons for the inefficacy of Triapine monotherapy against solid tumors are still unknown but might be fast metabolism/excretion[14] and/or ineffective drug delivery[15, 16]. Thus, novel strategies to increase tumor accumulation and specificity of thiosemicarbazones are of high interest.

Notably, also di(2-pyridyl)ketone thiosemicarbazones, such as di(2-pyridyl)ketone-4,4-dimethyl-3-thiosemicarbazone (Dp44mT)[17] or the cyclohexyl-analoque di-2-pyridylketone-4-cyclohexyl-4-methyl-3-thiosemicarbazone (DpC)[18] have shown promising anticancer activity in numerous preclinical studies. Excitingly, DpC recently entered clinical phase I trials for treatment of advanced solid tumors (NCT02688101) and additionally another novel thiosemicarbazone, 4-(2-pyridinyl)-2-(6,7-dihydro-8(5*H*)-quinolinylidene)hydrazide (COTI-2) is currently undergoing phase I evaluation for treatment of advanced or recurrent gynecologic malignancies (NCT02433626).

A promising approach to enhance tumor targeting is the so-called active targeting approach. In this strategy, a tumor-targeting moiety which selectively binds to receptors that are overexpressed in cancer cells is conjugated to the drug. Prominent examples are vitamins like folic acid[19, 20], biotin[21] or sugars[22]. Notably, glycoconjugation of thiosemicarbazones, targeting the increased expression of glucose transporters in colorectal cancer cells, has been described previously[23]. The biotin moiety is one of the best investigated targeting ligands with several literature examples proving evidence of its beneficial properties[24-26]. Biotin, which is also known as vitamin B_7 or coenzyme R, is an essential growth promotor at cellular level and works as a coenzyme for carboxylase enzymes in the preparation of fatty acids, valine and isoleucine. Additionally, it plays essential roles in cell signaling and epigenetic gene regulation[27]. The main transporter for biotin is the sodium-dependent multivitamin transporter (SMVT). While the biotin transport is widely referred to as Na^+-dependent[28], the exact mechanism is still in discussion and several modes of action have been proposed e.g. via ligated intestinal loops or isolated enterocytes[29]. Since the SMVT is

overexpressed in a broad range of cancer cell lines, biotin conjugates are taken up preferentially by these cells[30]. Consequently, functionalization of thiosemicarbazones with the biotin moiety should enhance cellular uptake and lead to accumulation in the tumor tissue.

In this study, we synthesized several biotin-thiosemicarbazone conjugates and evaluated the biological activity on a panel of biotin-expressing cancer cell lines to select the most promising candidate. Furthermore, metal complexes of this derivative with the biologically relevant metals ions iron(III) and copper(II) were synthesized and evaluated regarding their anticancer activity, physico- and electrochemical properties, and their interaction with relevant antioxidants. Additionally, *in vivo* experiments using CT-26 colon cancer-bearing mice were performed with biotin-conjugated Triapine.

Results

Synthesis and characterization

For conjugation of anticancer thiosemicarbazones to biotin three different derivatives were synthesized (Scheme 1): 1) **Triapine** conjugated via a butylene linker (**BioTriapine**), 2) 2-formylpyridine thiosemicarbazone (**FTCS**) conjugated via an ethylene linker (**BioFTSC1**) and 3) FTSC conjugated via a butylene linker (**BioFTSC2**). All derivatives were synthesized starting from the mono-tert-butyloxycarbonyl (BOC)-protected diamines, which were treated with CS_2, CH_3I and $N_2H_4 \cdot H_2O$ to the thiosemicarbazides. Subsequent condensation with the respective aldehyde and deprotection using conc. HCl generated the linker-containing thiosemicarbazones (**4a-c)**[31]. Finally, the NHS-ester of biotin was conjugated to obtain the desired biotin-

conjugated thiosemicarbazone derivatives **BioTriapine, BioFTSC1** and **BioFTSC2** with yields between 66 % and 84 %.

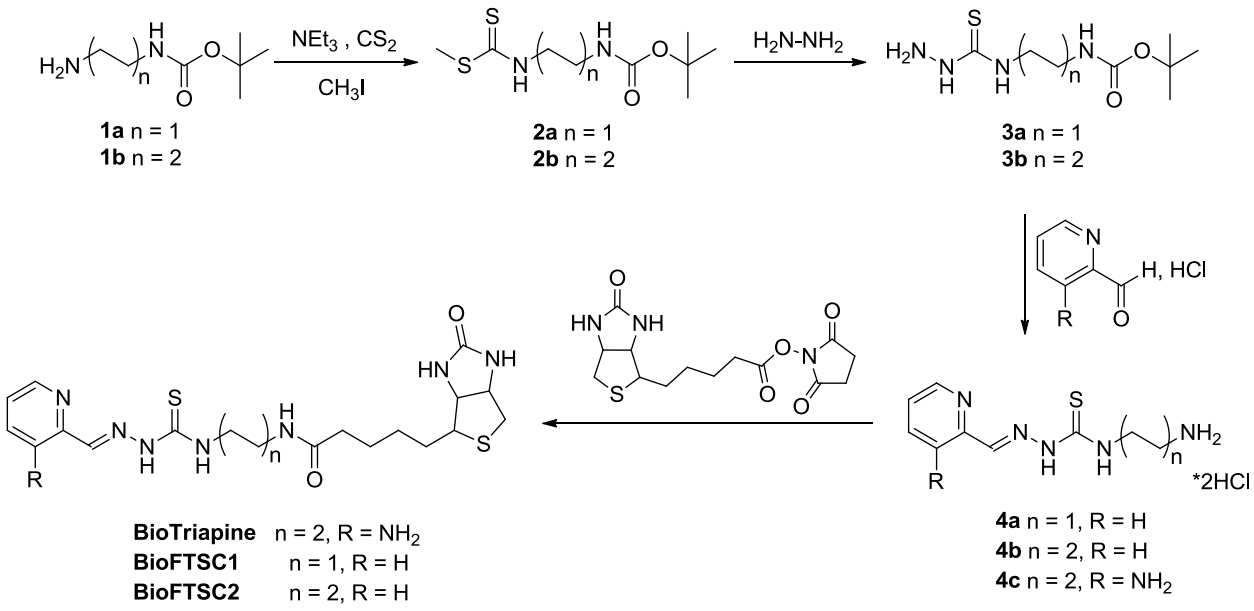

Scheme 1: Synthesis of the biotin-conjugated thiosemicarbazone derivatives **BioTriapine, BioFTSC1** and **BioFTSC2**

For **BioTriapine,** additionally, the respective copper(II) and iron(III) complexes were synthesized. In case of the copper complex, a 1:1 metal-ligand ratio was chosen (Figure 1) due to the generally low aqueous solubility of 1:2 complexes of the type [Cu(L_2)] (L representing mono-deprotonated thiosemicarbazone) and their tendency to at least partially dissociate into the corresponding 1:1 complexes at biologically relevant concentrations [32]. Reaction of **BioTriapine** with $CuCl_2 \cdot 2H_2O$ in MeOH at 1:1 ratio resulted in the formation of [Cu(BioTriapine)Cl_2]·H_2O (**Cu-BioTriapine**) in 81% yield. Negative ion electrospray ionization (ESI) mass spectra of this complex display a strong

main signal of $[M-2H-Cl]^-$ at *m/z* 588, as well as the $[M-H]^-$ signal at *m/z* 624, while in the positive mode the peak of $[M-2Cl-H]^+$ was found at *m/z* 554.

The iron complex $[Fe(BioTriapine)_2]NO_3$ (**Fe-BioTriapine**) was synthesized starting from $Fe(NO_3)_3 \cdot 9H_2O$ and **BioTriapine** in methanol in the presence of *N*-methylmorpholine. In case of iron(III) the bis complex was prepared to saturate the typical octahedral coordination sphere of this metal ion. Subsequent purification *via* RP-HPLC resulted in $[Fe(BioTriapine)_2]NO_3 \cdot 3.5H_2O$ with 42% yield. Positive ion ESI mass spectra for this complex show a sharp $[M]^+$ signal at *m/z* 1038. **Fe-Triapine** and **Cu-Triapine** were synthesized as described previously[33, 34].

Fe-BioTriapine

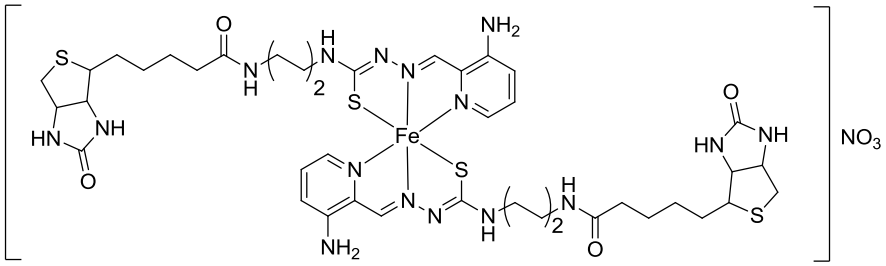

Cu-BioTriapine

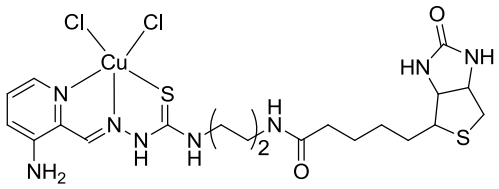

Fe-Triapine

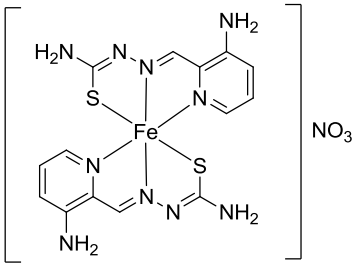

Cu-Triapine

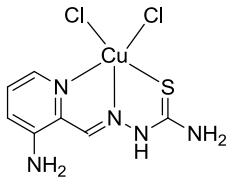

Figure 1: Chemical structures of the novel biotin-conjugated metal complexes **Fe-BioTriapine** and **Cu-BioTriapine**, as well as the reference compounds **Fe-Triapine** and **Cu-Triapine**.

Anticancer activity of the new compounds in cell culture after 72 h drug exposure

As a first step, an appropriate cell line panel for the testing of our novel biotin-conjugated compounds was selected. Thus, several cell lines were starved for 24 h followed by treatment with FITC-labeled biotin (25 µM) for 6 h and analyzed on their fluorescence intensity by flow cytometry (Figure 2). In line with available literature[35], MCF7 cells showed exceptionally high in biotin uptake, while SKBR-3 and MDA-MB-231 had medium biotin accumulation. HCT116 cells served as negative uptake control.

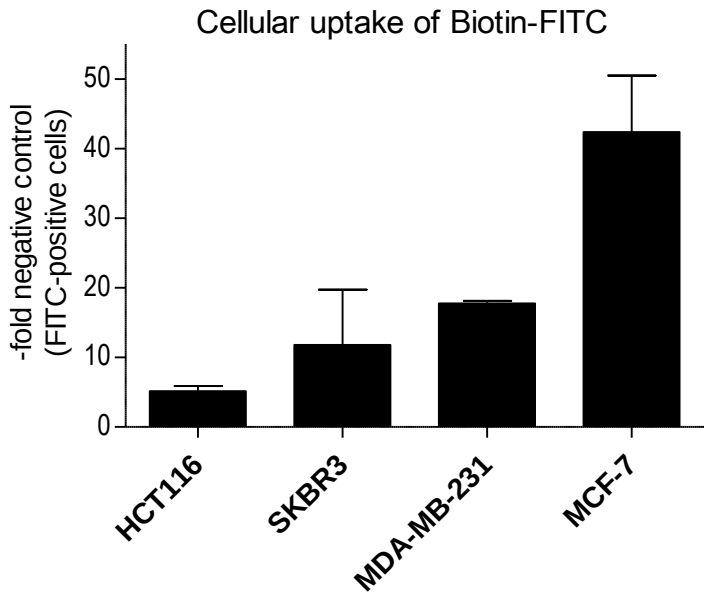

Figure 2. Uptake of FITC-labeled biotin in the cell line panel used in this study. The indicated cell lines were serum-starved for 24 h, followed by treatment with 25 µM FITC-labeled biotin for 6 h. Fluorescence was detected by flow cytometry. Values shown are means and standard deviation of three samples.

This cell line panel was then tested for their sensitivity against the biotin-conjugated thiosemicarbazones in comparison to the respective parental drugs (Table 1). With regard to the non-biotinylated drugs **Triapine** and **FTSC**, in general, all cell lines were similarly sensitive with an IC_{50} of ~ 1 µM and 3.5 µM, respectively. Only SKBR-3 cells were more resistant with a ~5-fold and 8-fold increased IC_{50} value, respectively. Also **Fe-Triapine** and **Cu-Triapine** widely followed this trend. With regard to the impact of biotin conjugation, no clear trends were visible. Thus, in case of **BioTriapine**, HCT116, MDA-MB-231 and MCF-7 have an IC_{50} value of ~ 3 µM. This would indicate that biotin-conjugation slightly decreases the anticancer activity of Triapine. However, in the thiosemicarbazone-resistant SKBR-3 model biotinylation of Triapine distinctly enhanced its efficacy. Interestingly, the comparison of **BioFTSC1** and **BioFTSC2** indicated that the chosen linker system strongly influences the anticancer activity, as the ethylene linker-containing derivative (**BioFTSC1**) was far less effective than the butylene linker-containing compounds (**BioFTSC2** and **BioTriapine**). With regard to the impact of metal coordination, highly unexpected results were obtained. Thus, Cu(II) as well as Fe(III) coordination strongly diminished the activity of **BioTriapine**. In case of Cu(II) complexation, especially in the SKBR-3 and MCF-7 cell line, up to ~30 fold reduced activity of **BioTriapine** was observed, in comparison **Triapine** complexation resulted in an only up to ~5 fold decrease. In HCT116 cells, the copper complexation of **Triapine** induced a stronger activity decrease as compared to **BioTriapine**. With regard to **Fe-BioTriapine**, the differences were even more striking with a complete inactivation up to the highest tested concentration of 100 µM in all cell lines, in strong contrast to **Fe-Triapine** with IC_{50} values of ~5 µM. Additionally, the activity of none of the new biotin-

conjugated compounds followed the uptake of FITC-labeled biotin in the initial experiments (compare Figure 2). A similar activity pattern was observed in the murine colon carcinoma CT-26 cell line, our routine screening model for subsequent *in vivo* studies (see below). In contrast, the non-malignant human fibroblasts HLF were much less sensitive to the compounds compared to most of the tested cancer cell models.

Table 1: IC_{50} values of the new compounds in comparison to Triapine and FTSC references after 72 h incubation. The compounds were tested in the indicated cell lines via MTT-based viability assays. The means of the IC_{50} values (expressed in µM) were calculated from at least two experiments.

Cell line	HCT116	MDA-MB-231	SKBR-3	MCF-7	CT26	HLF
Biotin Uptake	low	medium	medium	high	n.t.	n.t.
	IC_{50} ± SD	IC_{50} ± SD	IC_{50} ± SD	IC_{50} ± SD	IC_{50} ± SD	IC_{50} ± SD
Triapine	0.8 ± 0.4	1.5 ± 1.1	8.8 ± 0.6	1.0 ± 0.1	0.8 ± 0.2	> 10
BioTriapine	3.6 ± 0.1	3.2 ± 0.8	0.7 ± 0.3	2.9 ± 0.9	4.1 ± 1.2	7.6 ± 1.1
Cu-Triapine	7.8 ± 0.04	4.8 ± 0.2	6.5 ± 2.5	4.7 ± 0.1	5.2 ± 1.1	> 25
Cu-BioTriapine	19.3 ± 3.7	18.3 ± 0.8	19.1 ± 1.0	37.4 ± 4.5	> 100	> 100
Fe-Triapine	4.1 ± 0.8	3.9 ± 0.6	6.9 ± 2.6	4.4 ± 0.02	1.7 ± 1.0	4.3 ± 0.3
Fe-BioTriapine	> 100	> 100	> 100	> 100	> 100	> 100
FTSC	3.2 ± 0.002	3.6 ± 0.8	16.1 ± 1.3	3.9 ± 0.3	2.9 ± 0.9	> 25
BioFTSC1	31.4 ± 3.6	10.8 ± 0.7	63.2 ± 2.8	42.3 ± 8.6	> 75	56.1 ± 8.0
BioFTSC2	2.0 ± 0.3	8.6 ± 1.4	2.8 ± 0.4	2.7 ± 0.9	> 10	> 10

Anticancer activity of oral BioTriapine against murine CT26 colon carcinoma *in vivo*

In parallel to the cell culture experiments, first *in vivo* tests of **BioTriapine** were performed using CT-26 colon carcinoma-bearing mice. To this end, murine CT26 cells were injected into the right flank of Balb/c mice and oral treatment with **BioTriapine** (25 mg/kg) was started when the tumors were palpable. Therapy was well tolerated which

was also indicated by a stable body weight during treatment (data not shown). As shown in Figure 3, **BioTriapine** significantly retarded the tumor growth of CT-26 cells comparable to the reference compound **Triapine**.

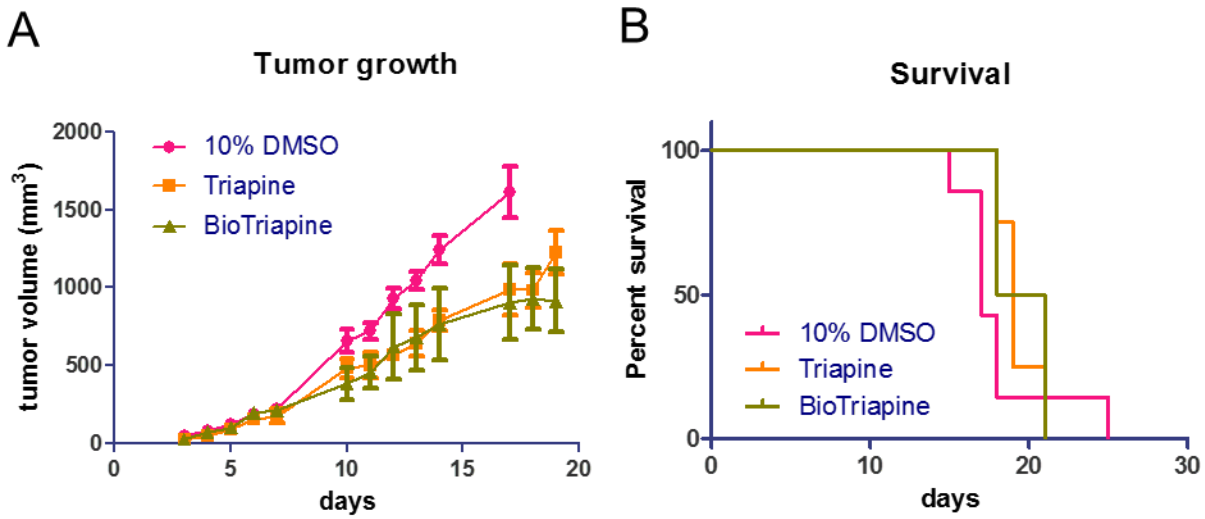

Figure 3. Anticancer activity *in vivo*. Murine CT-26 cells (5×10^5 cells in 50 µL) were injected subcutaneously into the right flank of Balb/c mice. Animals were treated with **BioTriapine** or **Triapine** orally (25 mg/kg in 10% DMSO) on days 3-7 and 10-14. Tumor size was assessed regularly by caliper measurement. Number of animals is 4 per group. **(A)** Tumor volumes (means ± standard errors of the mean, SEM), calculated using the formula: length × width^2 / 2. Tumors in **BioTriapine**-treated animals were significantly smaller in comparison to solvent-treated animals on day 17; two-way ANOVA *** $p<0.001$. **(B)** Overall survival of the **BioTriapine**-treated animals was significantly prolonged; Mantel-Cox test *$p<0.05$.

Impact of biotinylation on uptake of Cu-BioTriapine vs. Cu-Triapine and $CuCl_2$

Based on the distinctly decreased activity of the metal complexes of **BioTriapine**, we hypothesized that this could be based on reduced uptake of the biotinylated compounds. Consequently, to gain more insights into this issue, cellular copper levels of HCT116 and MCF7 cells were evaluated after treatment with **Cu-BioTriapine**, **Cu-Triapine** or $CuCl_2$ for 4 h using inductively coupled plasma mass spectrometry (ICP-MS; the measurement of the iron complexes was not possible due to the high environmental background levels of iron). Interestingly, although untreated HCT116 had slightly higher intrinsic levels of copper than MCF-7 cells, both cell models accumulated $CuCl_2$ to comparable extent (Figure 4). In general, MCF-7 cells were more active with regard to the uptake of both Cu thiosemicarbazones in comparison to HCT116 cells. Thus, in agreement with the viability data, biotin uptake levels (Figure 2) did not correlate with the intracellular levels of **Cu-BioTriapine**. At lower drug concentrations (25 µM), biotinylation of **Cu-Triapine** resulted in reduced intracellular levels, while at 50 µM there was a tendency for higher **Cu-BioTriapine** uptake compared to **Cu-Triapine.** In summary, there was no clear-cut trend between the two thiosemicarbazone, which could serve as explanation for the ~ 10-fold difference in IC_{50} value between these two drugs in MCF7 cells.

To evaluate the role of the SMVT in the drug uptake of our cancer cells, inhibition experiments using the SMVT inhibitor indomethacine were performed[36]. In contrast to the FITC-labelled biotin, where indomethacine treatment distinctly reduced uptake in MCF-7 but not HCT-116 cells, the inhibitor was not able to prevent the cellular accumulation of **Cu-BioTriapine** (or **Cu-Triapine**) (Figure 5).

This, on the one hand, indicates that the biotinylation of Cu-Triapine does not result in enhanced uptake in cells with higher biotin uptake and, on the other hand, does not explain the reduced activity of these drugs against cancer cells.

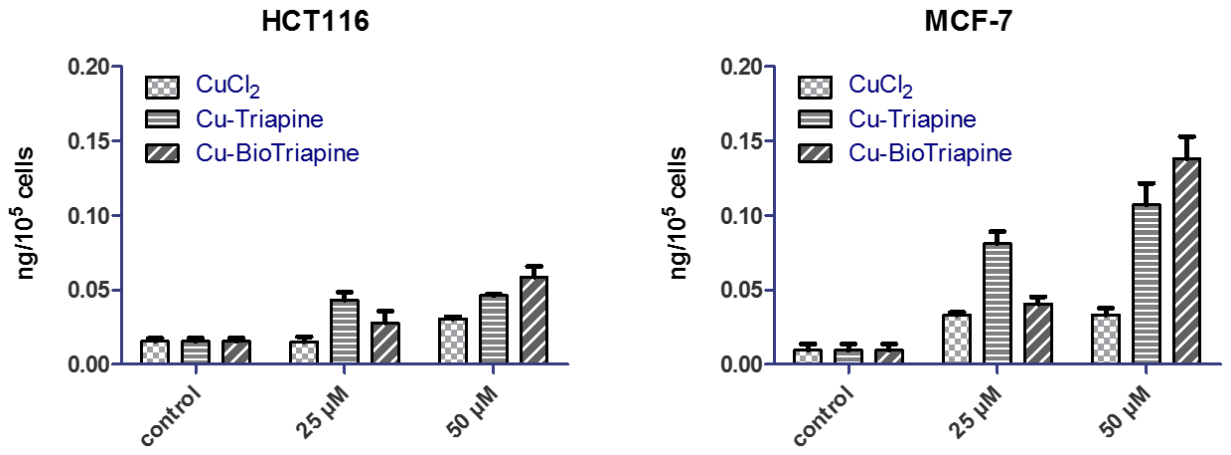

Figure 4. Cellular uptake of copper compounds. Cells were treated with **Cu-Triapine**, **Cu-BioTriapine** or **$CuCl_2$** (25 µM or 50 µM) and incubated for 4 h at 37°C. Intracellular copper levels were detected by ICP-MS measurements.

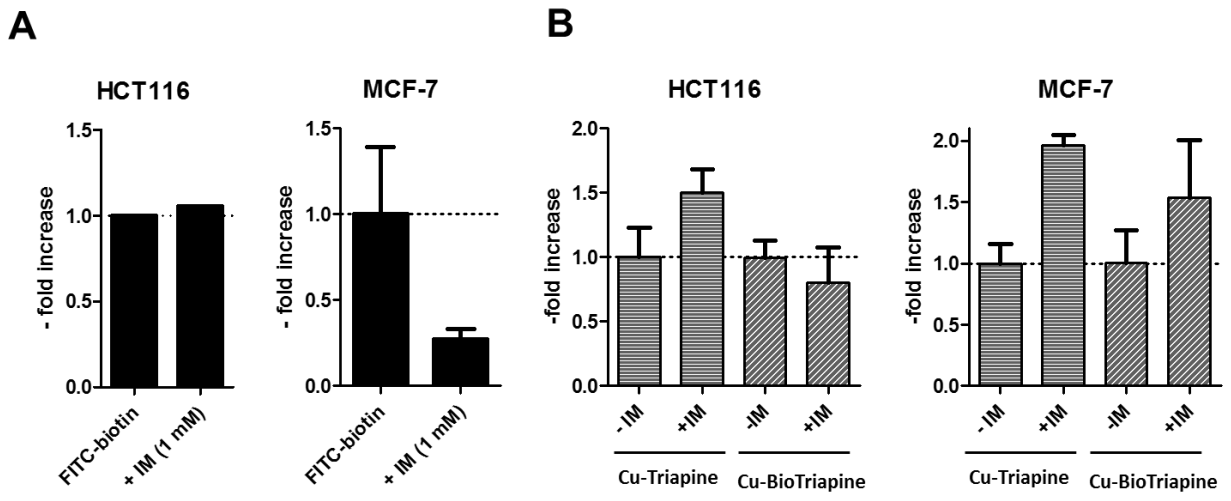

Figure 5. Impact of the SMVT inhibitor indomethacine on uptake of FITC-biotin and **Cu-BioTriapine**. The indicated cell lines were treated with A) FITC-biotin or B) **Cu-Triapine** and **Cu-BioTriapine** (25 µM) with and without 1 mM indomethacine (IM) and incubated for 4 h at 37°C. Uptake was measured by flow cytometry and ICP-MS, respectively.

Impact of long-term exposure on the anticancer activity of biotin thiosemicarbazone derivatives

Since the strong impact of biotinylation on the effectivity of metal-containing thiosemicarbazones could not be explained by changes in the cellular uptake, we hypothesized that the compounds need longer exposure time in order to get activated in a redox-dependent manner. Consequently, we wanted to know whether prolonged exposure time results in enhanced efficacy of the compounds. To this end, clonogenic assays with 9 days of exposure were performed in HCT116 and MCF7 cells.

As shown in Table 2, prolonged exposure time in general resulted in enhanced activity of the drugs against both cell models. Moreover, the increase in activity compared to the 72 h experiment was similar in both cell lines for **Triapine**, **BioTriapine**, **Cu-Triapine** and **Fe-Triapine.** However, in case of the biotinylated metal complexes distinct differences were observed: while **Cu-BioTriapine** was comparably active in MCF7 cells after 3 days and 9 days of exposure, the compounds distinctly lost their activity upon prolonged incubation time in HCT116 cells. In contrast, **Fe-BioTriapine** was distinctly activated by prolonged exposure time, especially in the MCF7 cells, however could by far not reach the levels of **Fe-Triapine**.

Table 2. IC_{50} values of the thiosemicarbazone compounds after 9 days of incubation. The compounds were tested in the indicated cell lines via clonogenic assays. The means of the IC_{50} values (expressed in µM) were calculated from at least two experiments. The table also shows a comparison of the results to the short term viability assays with 72 h incubation.

	HCT116		MCF-7	
	IC_{50} ± SD	**increase to 72 h**	**IC_{50} ± SD**	**increase to 72 h**
Triapine	0.4 ± 0.04	2.0-fold	0.4 ± 0.1	2.5-fold
BioTriapine	0.6 ± 0.2	6.0-fold	0.7 ± 0.1	4.1-fold
Cu-Triapine	1.6 ± 0.2	4.9-fold	0.9 ± 0.1	5.2-fold
Cu-BioTriapine	> 40	< 0.5-fold	31.7 ± 1.3	1.2-fold
Fe-Triapine	0.9 ± 0.02	4.6-fold	1.0 ± 0.1	4.4-fold
Fe-BioTriapine	62.8 ± 2.1	> 1.7-fold	28.8 ± 3.5	> 3.7-fold

Comparison of pK_a values and lipophilicity of Triapine and BioTriapine

Due to the surprisingly strong differences in the activity of the metal complexes of **BioTriapine** compared to the reference complexes of **Triapine** alone (especially the remarkably low activity of **Fe-BioTriapine**), we were interested if the metal complexes of **Triapine** and **BioTriapine** show different physico-chemical properties that might explain their different biological behaviour.

First of all the solution equilibrium properties of **BioTriapine** were studied in pure water using UV-visible (UV-vis) spectrophotomeric titrations. For adequate comparison, measurements were also performed for **Triapine** and its complexes under identical conditions (the proton dissociation processes of **Triapine** and its complexation with copper(II) and iron(III) ions were already reported in our previous works[7, 37], however, these measurements were performed in a 30% (w/w) DMSO/H_2O solvent mixture). The

pK_a values of the ligands (Table 3) were determined by the deconvolution of UV-vis spectra recorded in the pH range from 2 to 11.5. As expected, characteristic changes were seen in the UV-vis spectra of the ligands due to the deprotonation processes as shown for **BioTriapine** in Figure 6. **Triapine** and **BioTriapine** possess two dissociable protons, namely at the pyridinium (NH^+) nitrogen (pK_1) and the hydrazinic (NH) nitrogen of the thiosemicarbazide moiety (pK_2). In the latter deprotonation step the negative charge is mainly localized on the sulfur atom due to the thione–thiol tautomeric equilibrium in the completely deprotonated form of the ligands.

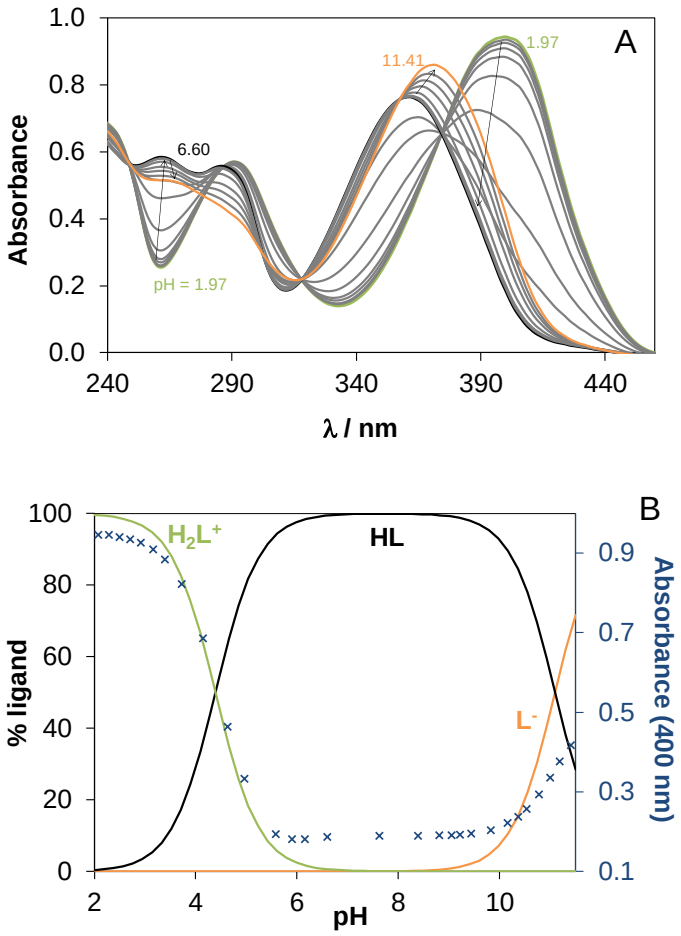

Figure 6. (A) UV-vis spectra of **BioTriapine** recorded at various pH values and **(B)** concentration distribution curves for the ligand species with the absorbance values at 400 nm. [c_L = *74 μM; pH = 2 – 11.5; T = 25 ˚C; I = 0.10 M (KCl);* ℓ *= 1.0 cm*]

Comparing the proton dissociation constants of the ligands (Table 3) it can be concluded that the *N*-terminally biotin derivatization results in somewhat elevated pK_a values. In comparison to **Triapine,** especially pK_2 is higher due to the close proximity of the electron donating biotin methylene groups to the deprotonating thiosemicarbazide moiety. Both ligands are charge-neutral (in HL form) at physiological pH. Notably, the lipophilicity of **BioTriapine**, expressed as n-octanol-water distribution coefficient at pH 7.4, is just slightly higher compared to that of **Triapine** (see log$D_{7.4}$ values in Table 3).

Solution stability of the copper(II) and iron(III) complexes of Triapine and BioTriapine

In order to characterize the aqueous solution behavior of **Cu-BioTriapine** and **Cu-Triapine**, they were dissolved in an acidic solution and titrated by strong base while their UV-vis spectra were recorded (see representative spectra for **Cu-BioTriapine** in Figure S1A). For both thiosemicarbazone complexes, the spectra revealed two well-separated equilibrium processes with increasing pH. Based on the findings reported in the presence of 30% (w/w) DMSO for the copper(II)-Triapine system[7], the first step in the acidic pH range is most likely the deprotonation of the complex $[CuLH]^{2+}$. Then the mixed hydroxido species [CuL(OH)] is formed from $[CuL]^{+}$ in the basic pH range. Therefore, pK_a values of $[CuLH]^{2+}$ and $[CuL]^{+}$ complexes were determined by the spectral data evaluation (Table 3) in addition to the individual spectra of the complexes

(Figure 6B). The pK_a values of the complexes are in the same range as reported by Antholine *et al.* in the case of 2-formylpyridine thiosemicarbazone (FTSC) (pK_a = 2.40 and 8.30) in aqueous solution (with 1% DMSO)[38].

Table 3. pK_a and log$D_{7.4}$ values of **Triapine** and **BioTriapine** and their various copper(II) complexes determined by spectrophotometric titrations, conditional (logβ') stability constants for $[CuL]^+$ species at pH 5.90 determined *via* EDTA displacement reaction and overall stability constants (logβ) in addition to pCu values and fractions of [CuL(OH)] at pH 7.4 (logβ) [t = 25 °C, I = 0.10 M (KCl)].

	Triapine	**BioTriapine**
pK_a (H_2L^+)	4.25±0.01	4.39±0.02
pK_a (HL)	10.58±0.01	11.10±0.02
pK_a $[CuLH]^{2+}$	2.51±0.08	2.55±0.08
pK_a $[CuL]^+$	8.64±0.08	8.71±0.06
log$\beta'_{5.9}$ $[CuL]^+$ [a]	12.88±0.06	12.97±0.07
logβ $[CuLH]^{2+}$ [b]	20.08	20.73
logβ $[CuL]^+$ [b]	17.57	18.18
logβ [CuL(OH)] [b]	8.93	9.47
pCu [c] at pH 7.4	11.35	11.50
% [CuL(OH)] at pH 7.4	5.4	4.7
log$D_{7.4}$	+0.85[d]	+0.95±0.06[e]

[a] Data for pK_a of EDTA and its Cu(II) complex taken from Ref.[39] and log$\beta'_{5.90}$ = 13.89 was calculated for $[Cu(EDTA)]^{2-}$. [b] β $[CuL]^+$ = β' $[CuL]^+ \times \alpha_H$, where $\alpha_H = 1 + [H^+]/K_a(HL) + [H^+]^2/ (K_a(HL) \times K_a(H_2L^+))$; $[H^+] = 10^{-5.90}$ M. Log β $[CuLH]^{2+}$ = log β $[CuL]^+$ + pK_a $[CuLH]^{2+}$. Log β [CuL(OH)] = log β $[CuL]^+$ – pK_a $[CuL]^+$. [c] pCu = −log [Cu(II)] at pH 7.40, $c_{Cu(II)} = c_L$ = 1 μM. [d] Taken from Ref.[6] [e] Data was determined using the same approach as in Ref.[6].

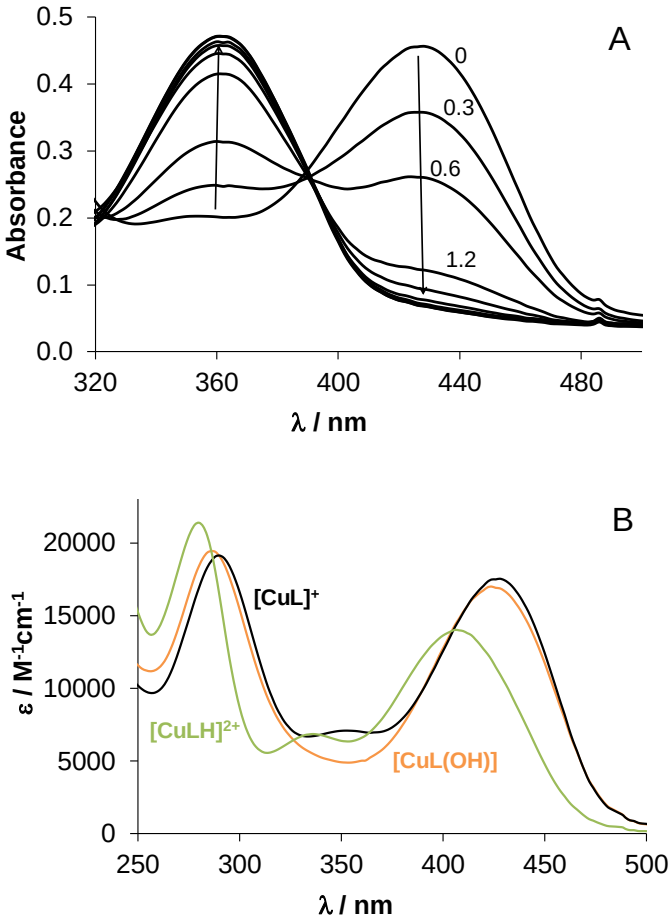

Figure 7. (A) UV-vis spectra of **Cu-BioTriapine** in the presence of EDTA at various concentrations (the numbers show the EDTA-to-complex ratios) [$c_{complex}$ = *25 μM; c_{EDTA} = 0-75 μM; pH = 5.90 (50 mM MES); T = 25 ˚C; I = 0.10 M (KCl); ℓ = 1.0 cm*] and (**B**) calculated individual absorption spectra of complex species of **Cu-BioTriapine**. [$c_{complex}$ = *25 μM; pH = 2 – 11.5; T = 25 ˚C; I = 0.10 M (KCl); ℓ = 1.0 cm*]

The apparent (conditional) formation constants (*β′*) for this type of complexes of **Triapine** and **BioTriapine** were determined by competition reactions with EDTA spectrophotometrically at pH 5.90. The displacement by EDTA is not instantaneous and it was found that during a 2 h waiting time the equilibrium state could be reached for the competition reaction. Representative UV-vis spectra are shown for the copper(II)

complex of **BioTriapine** in the presence of EDTA at various concentrations (Figure 7A). EDTA and its copper(II) complex have negligible contribution to the measured absorbance values in the monitored wavelength range (320–550 nm) and merely species $[CuL]^+$ and HL absorb light. The increasing amount of EDTA results in decrease in the absorbance at the wavelength 422 nm at which the transition belongs to the characteristic S→Cu charge-transfer band (Figure S1B). The determined conditional formation constants are collected in Table 3. From these data the overall stability constants (β) of the complexes $[CuL]^+$, $[CuLH]^{2+}$ and [CuL(OH)] were calculated. These constants reveal that $[CuL]^+$ is the predominating species at physiological pH and the fraction of [CuL(OH)] is low (~ 5%). The pCu (−log [Cu(II)]) values were also calculated using the experimentally determined equilibrium constants in order to compare the copper(II) binding ability of the ligands at physiological pH (Table 3), as the direct comparison of the logβ $[CuL]^+$ constants is not adequate due to the somewhat different basicity of the ligands. All these data confirm the fairly similar solution stability of the copper(II) complexes of **Triapine** and **BioTriapine**. Notably, the solution stability of the **Triapine** copper(II) complex is higher in pure water compared to that showed in the 30% (w/w) DMSO/H_2O mixture, as it was expected, since DMSO can coordinate to copper(II) very weakly.

The same competition reaction with EDTA was performed for the iron(III) complexes of **Triapine** and **BioTriapine**. However, it was found that even a 60-fold excess of EDTA could not replace the original ligand after 2 h, and even after 48 h only a minor spectral change could be detected. This finding suggests a kinetically rather inert character of these iron(III) complexes that hinders the accurate determination of

the conditional stability constants. Nevertheless, the data suggests that both iron(III) complexes show very high stability. The high stability was also reflected in the experimental finding that acidification of both iron(III) complexes down to pH 2 did not lead to the complex dissociation (at 20 µM concentration in pure water).

Redox behavior of the copper(II) and iron(III) complexes

Since the stability measurements did not show any significant differences between the copper(II) and iron(III) complexes of **Triapine** and **BioTriapine**, we performed electrochemical measurements to evaluate the redox behavior of the metal complexes. Cyclic voltammograms of **Fe-Triapine**, **Fe-BioTriapine**, **Cu-Triapine** and **Cu-BioTriapine** were measured in DMF/PBS pH 7.4 (2:1 v/v) containing 0.10 M [*n*-Bu_4N][BF_4] as supporting electrolyte (due to the low aqueous solubility of the complexes, measurements were performed in DMF/PBS mixtures). **Cu-Triapine** displayed an irreversible Cu(II)/Cu(I) reduction peak at E_p = –0.19 V versus normal hydrogen electrode (NHE) at 200 mV/s scan rate (in accordance with our previous reports[33]), while **Cu-BioTriapine** was reduced at E_p = –0.23 V. The slightly lower redox potential of **Cu-BioTriapine** in comparison to **Cu-Triapine** is in line with the electron donor properties of the methylene groups of the linker moiety. Interestingly, in contrast, both **Fe-Triapine** and **Fe-BioTriapine** have a reversible Fe^{III}/Fe^{II} redox couple at $E_{1/2}$ = +0.06 V. Consequently, the redox potential seems not to be a critical parameter when searching for distinct differences of the metal complexes. However, distinctions in the electrochemical properties of a compound can not only occur due to variations of the redox potential, but also in the kinetics of the reduction processes. Consequently,

we investigated the reduction behavior of the copper(II) and iron(III) complexes with the biologically important reducing agents ascorbic acid (AA) and glutathione (GSH). The reduction processes were followed for 20 min by UV-vis spectrophotometry in PBS at pH 7.4 using 20 eq. of reducing agent (the reducing agents itself and their oxidized forms mainly absorb at λ <~300 nm[40, 41], therefore the spectra are depicted in the range of 300–700 nm). AA practically was not able to reduce **Cu-Triapine** under the applied conditions (Figure S2A), whereas in case of **Cu-BioTriapine** a slow absorbance decrease at λ_{max} (426 nm) was observed (Figure 8A). Therefore, both copper(II) complexes could not be reduced efficiently by AA under the applied conditions which is in agreement with literature data of copper(II)-FTSC[42]. GSH is a more powerful reducing agent with a lower formal potential compared to that of AA (AA; +0.06 V vs. NHE[43]; GSH: –0.24 V vs. NHE[43]). As expected, GSH was able to reduce both copper(II) complexes (Figures 8B and S2B). Notably, the first recorded spectrum after mixing the reactants showed a shift of the λ_{max} value (*e.g.* 426 → 432 nm for **Cu-BioTriapine**) most probably due to the formation of a ternary complex with GSH. Subsequently, a significant decrease of the absorbance was observed at this λ_{max}, while the absorbance value was increased at the λ_{max} of the free ligand (~360 nm), which most probably can be explained by the formation of the unstable copper(I) complex with subsequent dissociation of the free ligand. The reaction seems to be incomplete in both cases since no further changes in the spectra occurred after ~10–15 min (Figures 8B and S2B). To prove that a complete reduction of the copper(II) complexes indeed generates the free ligands, dithiothreitol (DTT) with a redox potential of –0.33 V[44] was used. Co-incubation with DTT resulted in complete loss of the maximum of the

copper(II) complex at ~420 nm and an instant formation of a new band at λ_{max} ~360 nm, identical with the spectra of the free ligands (Figures 8C and S2C).

Notably, comparison of the reduction rate of **Cu-BioTriapine** and **Cu-Triapine** in the presence of GSH by plotting $\ln(A/A_0)$ vs. t (Figure 8D using the absorbance at 432 nm) indicated that the reduction is slower and less complete for **Cu-BioTriapine** compared to **Cu-Triapine**.

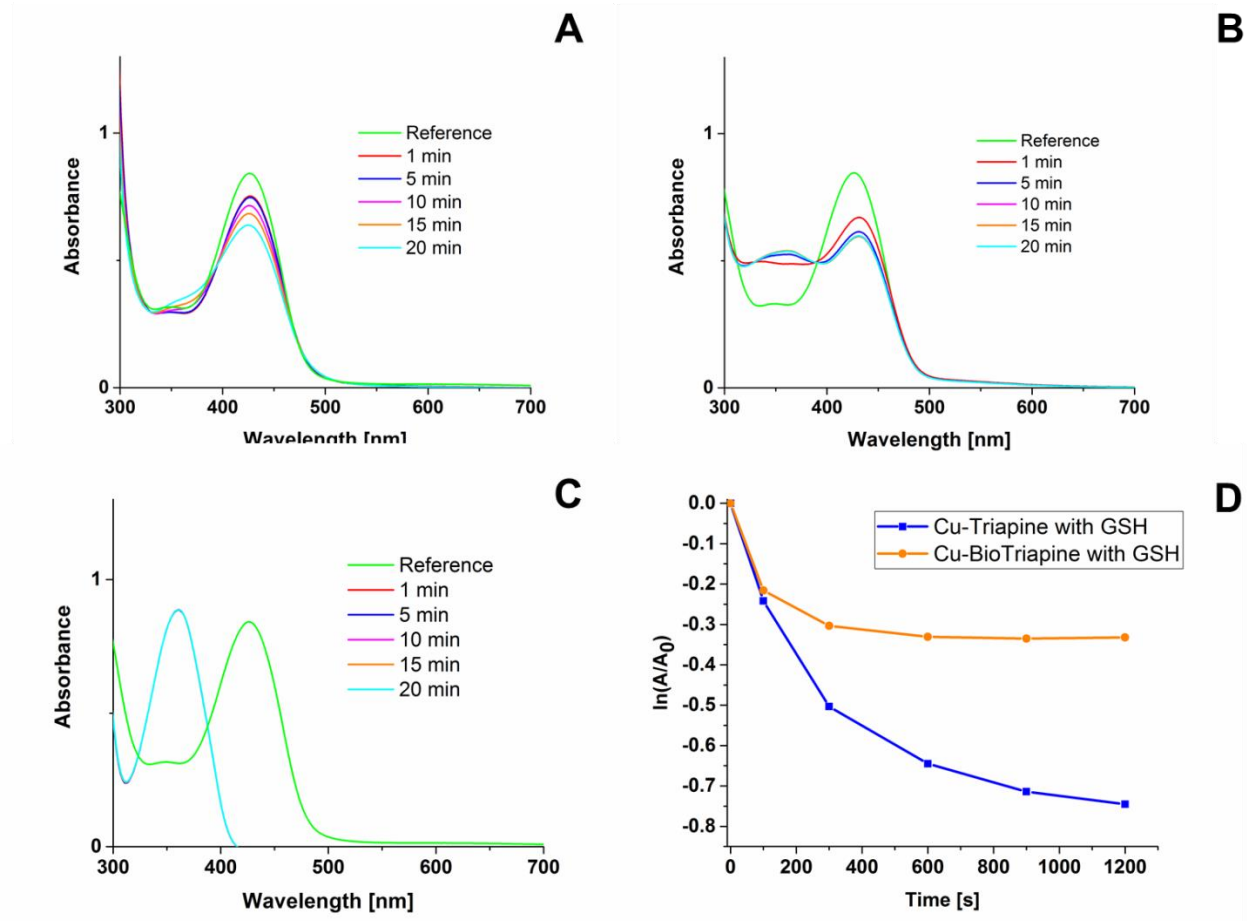

Figure 8. Time-dependent UV-Vis spectra of **Cu-BioTriapine** after addition of 20 equiv. **(A)** AA, **(B)** GSH and **(C)** DTT. ('reference' indicates the spectra of **Cu-BioTriapine** without reducing agent while '1 min' represents the spectrum measured directly after addition of the reducing agent). (**D)** The ln (A/A_0) values recorded at 432 nm were plotted against the time for the reduction of **Cu-Triapine** (blue line) and **Cu-BioTriapine** (orange line) with 20 equiv. GSH.

In the case of the iron(III) complexes all three reductants were able to reduce the complexes, in line with the higher redox potential compared to the copper(II) complexes. Reduction led to the development of novel bands in the spectra at 500–650 nm being characteristic for the greenish iron(II) species (Figure S3A-E). In the case of the reduction of **Fe-BioTriapine** with DTT, a precipitate was formed making adequate monitoring of the reduction process complicated. Generally, reduction was instantaneous with AA and DTT, while it was somewhat slower with GSH (Figures S3B and S3E). Evaluation of the reduction speed with GSH revealed as in case of the copper(II) complexes that **Fe-BioTriapine** is reduced slightly slower compared to **Fe-Triapine** (data not shown).

H_2O_2 and superoxide radical formation ability of the metal complexes

It is well-known that especially copper(II) complexes of thiosemicarbazones (including **Cu-Triapine**) are able to redox cycle with formation of H_2O_2 and $O_2^{\cdot-}$[33, 45], which could also be influenced by differences in the reduction kinetics. To examine whether this is applicable also for the new **BioTriapine** complexes, the metal complexes were co-incubated with AA and *N*-acetylcysteine (NAC) under cell-free conditions and H_2O_2 levels were determined using the xylenol-based PerOXOquant assay. As depicted in Figure 9A, the iron complexes did not induce significant H_2O_2 production. In contrast, co-incubation of the copper complexes with NAC resulted in high levels of H_2O_2 formation (~2 equiv. of H_2O_2 per copper complex) in line with previous data on **Cu-**

Triapine[33]. As expected from the co-incubation reduction experiments co-treatment with AA could not generate relevant levels of H_2O_2.

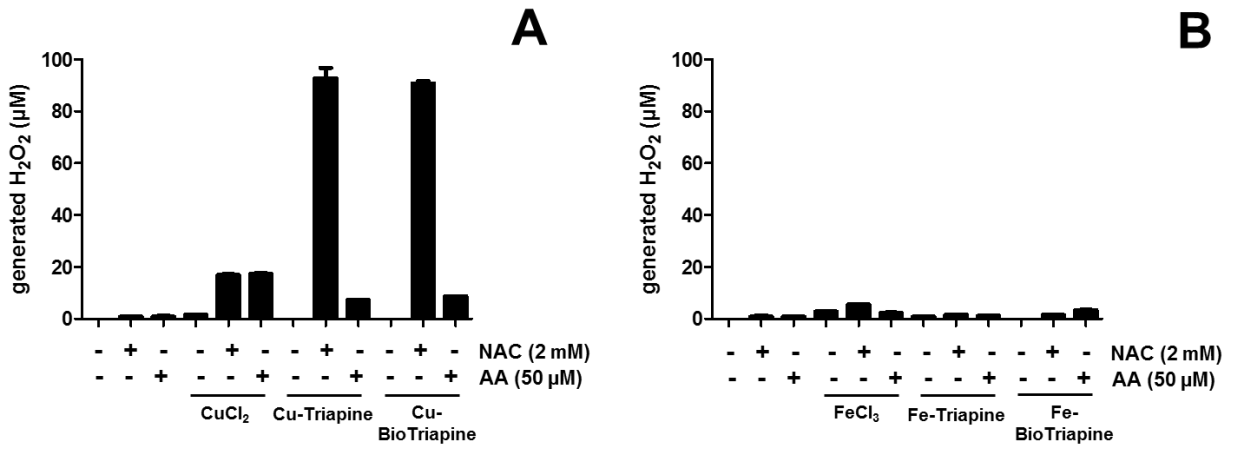

Figure 9: NAC- and AA-induced H_2O_2 production of **(A)** copper(II) and **(B)** iron(III) complexes of **Triapine** and **BioTriapine** determined using the xylenol-based PerOXOquant assay. The metal complexes were used at concentrations of 50 µM and the reducing agents at 2 mM (NAC) and 50 µM (AA). The results given are the mean ± standard deviation of three determinations.

To investigate the ability of the metal complexes to generate $O_2^{\cdot -}$ upon reduction by NAC or AA, nitroblue tetrazolium (NBT) was used as an $O_2^{\cdot -}$ detecting agent. As depicted in Figure 10A, distinct formation of $O_2^{\cdot -}$ was detected for the copper(II) complexes in the presence of NAC, while in presence of AA no $O_2^{\cdot -}$ formation was detected as expected. In case of the iron(III) complexes **Fe-BioTriapine** and **Fe-Triapine**, both AA and NAC induced formation of $O_2^{\cdot -}$ (Figure 10B), which is also in accordance with reduction data (Figure S3). Interestingly, $O_2^{\cdot -}$ generation by co-incubation with AA was distinctly lower with **Fe-BioTriapine** than with **Fe-Triapine**.

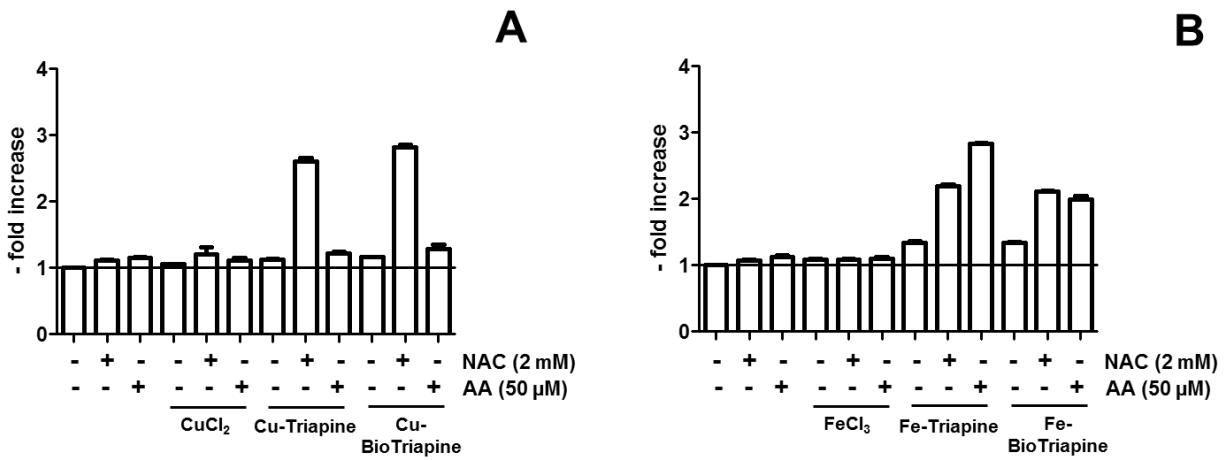

Figure 10: $O_2^{\bullet-}$ generation ability of **(A)** copper(II) and **(B)** iron(III) complexes of **Triapine** and **BioTriapine** in the presence of NAC and AA. The dependency of the level of generated $O_2^{\bullet-}$ on NAC (2 mM) and AA (50 µM) was determined by measuring the reduction of nitroblue tetrazolium (NTB) spectrophotometrically. The metal complexes were used at concentrations of 25 µM. The values given are the mean ± standard deviation of three determinations.

Discussion

Triapine is a prominent anticancer drug candidate which has already been investigated in more than 30 clinical phase I and II trials[8, 10]. However, at least partially based on insufficient tumor accumulation, further development into clinical phase III has not been achieved so far[2]. Therefore, drug targeting is a very promising approach for this substance class to improve tumor accumulation and antitumor efficiency. In recent years, biotin-targeting has emerged as a prominent strategy to improve activity of anticancer drugs with several examples reported in literature[24, 26, 46]. Consequently, we synthesized novel thiosemicarbazone derivatives via biotin conjugation at the terminal nitrogen atom. Additionally, for the biotinylated Triapine derivative (**BioTriapine**) the respective iron(III) and copper(II) complexes were synthesized. Unexpectedly, subsequent *in vitro* activity evaluation of **BioTriapine** and the metal complexes **Cu-BioTriapine** and **Fe-BioTriapine** showed no correlation with the biotin uptake of the used cell lines. Furthermore, inhibition of the SMVT did not prevent cellular accumulation of Cu-**BioTriapine**. Notably, also several literature reports do not show a correlation of the cytotoxic activity of the biotin-conjugates and the biotin uptake ability[47-49]. On the other hand, in case of a gemcitabine-coumarin-biotin conjugate preferred uptake in a biotin receptor-positive cell line was proven by confocal microscopy[24]. Also a 5′-deoxy-5-fluorouridine derivative with two biotin moieties attached showed a good correlation with biotin uptake[46]. Analyzing the structure of the different conjugates, it seems that the derivatives with no or shorter linker moieties between the drug and the biotin carboxylic acid reveal insufficient correlations of

cytotoxicity and biotin uptake ability, whereas long spacers or double biotin-conjugation enabled biotin-dependent activity.

In the here presented study, generally both the coordination with Cu(II) as well as Fe(III) strongly diminished the activity of **BioTriapine** much stronger compared to the non-biotinylated **Triapine**. Notably, in long-term clonogenic studies the activity difference between **Cu-BioTriapine** and **Cu-Triapine** even increased in comparison to the results from 72 h experiments. Noteworthy, previous studies reported different activity changes of thiosemicarbazones after Cu(II) complexation, depending on the exact nature of the ligand and also the type of the used cell lines[32, 33]. For example, the activity of Cu-FTSC was increased ~3-fold in comparison to free FTSC, whereas APTSC (3-aminopyridine-2-carboxyaldehyde-^{4}N,^{4}N-dimethylthiosemicarbazone) showed ~15-fold decreased cytotoxicity after copper coordination[33]. Furthermore, copper coordination of 2-acetylpyridine-4,4-dimethyl-3-thiosemicarbazone and 2-acetylpyridine 4,4-dimethyl-3-thiosemicarbazone led to ~2-fold activity increase in the SK-N-MC cell line after 24h [32]. Consequently, the up to ~30 fold decreased cytotoxic activity is remarkable in case of **BioTriapine.** Astonishingly, complexation of **BioTriapine** with iron(III) resulted in complete inactivation of the ligand on all tested cell lines after 72 h. This is surprising as previous studies on iron(III) complexes of similar thiosemicarbazones reported generally only slightly decreased activities of the complexes in comparison to the free ligands[34, 50]. Further long-term cytotoxicity studies of **Fe-BioTriapine** resulted in an increased effectivity compared to the results after 72 h. However, **Fe-BioTriapine** was still ~30-40 times less active than **Fe-Triapine**. To exclude that altered uptake is responsible for the decreased activity of the biotinylated derivatives, the cell uptake of **Cu-BioTriapine**

compared to **Cu-Triapine** was investigated by ICP-MS measurements (the Fe(III) complexes could not be measured due to the very high iron background). However, these data did not show significant differences between **Cu-Triapine** and **Cu-BioTriapine** and therefore does not explain their strongly different cytotoxic activity. Consequently, we performed detailed physico- and electrochemical experiments to elucidate possible differences. However, neither lipophilicity or complex stability, nor the reduction potential or behavior in presence of reducing agents (like AA, GSH) of the metal complexes showed any striking differences between **BioTriapine** and **Triapine**. Only the reduction kinetics of the metal complexes in case of **BioTriapine** was slower. As there are several reports that copper(II) complexes of thiosemicarbazones induce H_2O_2 and superoxide formation[33, 45], we further investigated their generation in cell-free assays. However, distinct differences in this regard were not found either between **Cu-BioTriapine** and **Cu-Triapine** or between **Fe-BioTriapine** and **Fe-Triapine**, except reduced $O_2^{\cdot -}$ formation in the presence of AA in case of **Fe-BioTriapine**. Consequently, a strong contribution of altered reduction kinetics and by this formation of reactive oxygen species seems unlikely.

Although the biotin-conjugated thiosemicarbazones have been extensively investigated in this study by physico- and electrochemical methods, the striking cytotoxic activity differences between the **BioTriapine** metal complexes and that of **Triapine** could actually not be explained by their physicochemical properties. Consequently, differences in their biological functionality have to underlie the observed effects. One hypothesis could be that in case of the **BioTriapine** metal complexes the intracellular distribution is strongly altered resulting in insufficient target inhibition. On the other

hand, the bulky structures of **Cu-BioTriapine** and especially **Fe-BioTriapine** can lead to retention of the complexes in the cell membrane which prevents effective delivery into the cell and results in the significantly decreased activity. This effect could not be excluded by the performed ICP-MS uptake studies of the copper complexes.

Noteworthy, although the metal complexes revealed an unexpectedly low cytotoxic potential on cancer cell lines *in vitro*, **BioTriapine** as a metal-free ligand, showed significant tumor growth retardation in a CT-26 colon cancer mouse model comparable to **Triapine**. Therefore, biotin-conjugation of thiosemicarbazones is still an interesting strategy for future investigations. Keeping the distinct difference in the anticancer activity between the ethylene linker containing **BioFTSC1** and butylene-linker compound **BioFTSC2** in mind, a further increase of this linker between biotin and the thiosemicarbazone, e.g. even with a (mini-)PEG moiety, might be a promising option for structural modification in order to further increase the anticancer activity and probably also enable biotin-mediated selective accumulation.

Materials and Methods

1a was purchased from Alfa Aesar (Germany). **1b**[51], **2a**[52], **3a**[52], **2b**[31], **3b**[31], biotin-NHS[53], **Triapine**[34], **Fe-Triapine**[34] and **Cu-Triapine**[33] were synthesized according to literature. All other reagents and solvents were obtained from commercial suppliers and used without further purification. Elemental analyses were performed on a Perkin Elmer 2400 CHN Elemental Analyzer by the Microanalytical Laboratory of the University of Vienna. ESI-MS spectrometry was carried out with a Bruker HCT plus ESI-QIT spectrometer (Bruker Daltonic, Bremen, Germany). Expected and experimental isotope distributions were compared. ^{1}H and ^{13}C NMR spectra were recorded in d_6-DMSO or D_2O with a Bruker Avance III 500 MHz spectrometer at 500.10 (^{1}H) and 125.75 (^{13}C) MHz at 298 K. Chemical shifts (ppm) were referenced internal to the solvent residual peaks. For the description of the spin multiplicities the following abbreviations were used: s = singlet, d = duplet, t = triplet, q = quartet, m = multiplet.

Synthesis

(*E*)-*N*-(2-aminoethyl)-2-(pyridin-2-ylmethylene)hydrazine-1-carbothioamide dihydrochloride (4a). Compound **3a** (2.15 g, 9.18 mmol) was dissolved in ethanol (40 mL) and 2-formylpyridine (0.87 mL, 9.18 mmol) was added. The reaction mixture was stirred for 10 min at 90°C, concentrated HCl (3.78 mL) was added and the solution was refluxed for 4 h. After cooling to room temperature, the yellow precipitate was filtered off, washed with cold ethanol and dried in *vacuo*. Yield: 2.18 g (80 %). ESI-MS in methanol (positive): *m/z* 224 $[M+H]^+$. ^{1}H NMR (D_2O): δ = 8.67 (d, ^{3}J = 5 Hz, 1H, H_{py}),

8.48 (t, ^{3}J = 7 Hz, 1H, H_{py}), 8.10 (d, ^{3}J = 8 Hz, 1H, H_{py}), 8.07 (s, 1H, HC=N), 7.89 (t, ^{3}J = 8 Hz, 1H, H_{py}), 3.99 (t, ^{3}J = 6 Hz, 2H, NHCH_2), 3.28 (t, ^{3}J = 6 Hz, 2H, NHCH_2) ppm. ^{13}C NMR (D_2O): δ 178.7 (C=S), 147.1 (C_{py}), 145.5 ($C_{q,\ py}$), 142.3 (C_{py}), 133.4 (HC=N), 126.9 (C_{py}), 126.8 (C_{py}), 41.2 (NH*C*H_2), 39.0 (*C*$H_2$$NH_2$).

(*E*)-*N*-(4-aminobutyl)-2-(pyridin-2-ylmethylene)hydrazine-1-carbothioamide dihydrochloride (4b). Compound **3b** (0.30 g, 1.14 mmol) was dissolved in ethanol (4 mL) and 2-formylpyridine (0.11 mL, 1.14 mmol) was added. The reaction mixture was stirred for 10 min at 90°C, concentrated HCl (0.47 mL) was added and the solution was refluxed for 4 h. After cooling to room temperature, the solution was stored at 4°C overnight. The yellow precipitate was filtered, washed with cold ethanol and dried in *vacuo*. Yield: 0.34 g (92 %). ESI-MS in methanol (positive): *m*/*z* 252 $[M+H]^+$. ^{1}H NMR (D_2O): δ = 8.69 (d, ^{3}J = 6 Hz, 1H, H_{py}), 8.51 (ddd, ^{3}J = 8 Hz, ^{3}J = 8 Hz, ^{4}J = 2 Hz, 1H, H_{py}), 8.11 (d, ^{3}J = 8 Hz, 1H, H_{py}), 8.07 (s, 1H, HC=N), 7.93–7.90 (m, 1H, H_{py}), 3.69 (t, ^{3}J = 7 Hz, 2H, NHCH_2), 3.02 (t, ^{3}J = 7 Hz, 2H, NHCH_2), 1.78–1.67 (m, 4H, CH_2(CH_2)$_2$$CH_2$) ppm. ^{13}C NMR ($D_2O$): δ 176.9 (C=S), 146.8 (C_{py}), 145.6 ($C_{q,\ py}$), 142.3 (C_{py}), 133.1 (HC=N), 126.7 (C_{py}), 126.6 (C_{py}), 43.5 (NH*C*H_2), 39.1 (*C*$H_2$$NH_2$), 25.2 (-*C*$H_2$-), 24.0 (-*C*$H_2$-) ppm.

(*E*)-*N*-(4-aminobutyl)-2-((3-aminopyridin-2-yl)methylene)hydrazine-1-carbothioamide dihydrochloride (4c). (2-formyl-pyridin-3-yl)-carbamic acid tert-butyl ester (0.51 g, 2.28 mmol) and concentrated HCl (0.6 mL) were added to a solution of

compound **3b** (0.60 g, 2.28 mmol) in ethanol (12 mL). The solution was refluxed for 4 h and after cooling to room temperature the orange precipitate was filtered, washed with cold ethanol and dried in *vacuo*. Yield: 0.61 g (79 %). ESI-MS in methanol (positive): *m*/*z* 267 $[M+H]^+$. ^{1}H NMR (D_2O): δ = 8.22 (s, 1H, HC=N), 7.99 (dd, ^2J = 4 Hz, ^3J = 1 Hz, 1H, H_{py}), 7.78 (d, ^3J = 9 Hz, 1H, H_{py}), 7.60 (dd, ^2J = 9 Hz, ^3J = 5 Hz, 1H, H_{py}), 3.67 (t, ^3J = 6 Hz, 2H, NHCH_2), 3.01 (t, ^3J = 7 Hz, 2H, CH_2NH), 1.76–1.66 (m, 4H, CH_2(CH_2)$_2$$CH_2$) ppm. ^{13}C NMR ($D_2O$): δ 176.5 (C=S), 145.7 ($C_{q,\ py}$), 134.5 (HC=N), 132.1 (C_{py}), 131.1 (C_{py}), 126.6 (C_{py}), 126.5 (C_{py}) 43.6 (NH*C*H_2), 39.2 (*C*$H_2$$NH_2$), 25.4 (-*C*$H_2$-), 24.0 (-*C*$H_2$-) ppm.

(*E*)-5-(2-oxohexahydro-1*H*-thieno[3,4-*d*]imidazol-4-yl)-*N*-(2-(2-(pyridin-2-ylmethylene)hydrazine-1-carbothioamido)ethyl)pentanamide (BioFTSC1). A solution of biotin-NHS (0.10 g, 0.29 mmol) in abs. DMF (3 mL) was added to a suspension of **4a** (0.09 g, 0.29 mmol) and Et_3N (0.12 mL, 0.87 mmol) in abs. DMF (2 mL). After stirring of the reaction mixture overnight, water (15 mL) was added and the mixture was stored at +4°C for 15 min. Subsequently, the white precipitate was filtered off, washed with water/isopropanol (1:1 v/v) and dried in *vacuo*. The product was recrystallized from water. Yield: 0.18 g (66 %). Anal. Calcd for $C_{19}H_{27}N_7O_2S_2 \cdot H_2O$ (M_r = 467.61 g/mol): C, 48.80; H, 6.25; N, 20.97; S, 13.71. Found: C, 48.61; H, 6.19; N, 20.86; S, 13.55. ESI-MS in methanol (positive): *m*/*z* 450, $[M+H]^+$. ^{1}H NMR (500.10 MHz, DMSO-d_6): δ 11.76 (s, 1H, (C=N)NH), 8.81 (t, ^3J = 5 Hz, 1H, (C=S)N*H*CH_2), 8.60–8.55 (m, 1H, H_{py}), 8.38 (d, ^3J = 6 Hz, 1H, H_{py}), 8.10–8.06 (m, 2H, HC=N and CH_2NHC=O), 7.86 (ddd, ^3J = 8 Hz, ^3J = 8 Hz, ^4J = 2 Hz, 1H, H_{py}), 7.39 (ddd, ^3J = 7 Hz, ^3J = 5 Hz, ^4J

= 1 Hz, 1H, H_{py}), 6.40 (s, 1H, *H*N(C=O)NH), 6.35 (s, 1H, HN(C=O)N*H*), 4.30–4.26 (m, 1H, *H*C-CH), 4.10–4.06 (m, 1H, HC-C*H*), 3.62–3.56 (m, 2H, (C=S)NHCH_2CH_2NH), 3.35 (2H, (C=S)NHCH_2CH_2NH, partially below the water signal), 3.06–3.00 (m, 1H, CHS), 2.79 (dd, ^2J = 12 Hz, ^3J = 5 Hz, 1H, SCH_2), 2.55 (d, ^2J = 12 Hz, 1H, SCH_2), 2.12 (t, ^3J = 7 Hz, 2H, (C=O)CH_2CH_2CH_2CH_2), 1.62–1.23 (m, 6H, (C=O)CH_2CH_2CH_2CH_2) ppm. ^{13}C NMR (125.81 MHz, DMSO-d_6): δ 178.0 (C=S), 173.6 (NH(*C*=O)CH_2), 163.2 (HN(C=O)NH), 153.9 ($C_{q,\ py}$), 149.8 (C_{py}), 142.7 (HC=N), 136.9 (C_{py}), 124.6 (C_{py}), 120.7 (C_{py}), 61.5 (H*C*-CH), 59.6 (HC-*C*H), 55.8 (CHS), 45.0 ((C=S)NH*C*H_2CH_2NH), 40.0 (S-CH_2), 38.2 ((C=S)NHCH_2*C*H_2NH), 35.6 ((C=O)*C*H_2CH_2CH_2CH_2), 28.6, 28.5 and 25.6 ((C=O)CH_2*C*H_2*C*H_2*C*H_2).

(*E*)-5-(2-oxohexahydro-1*H*-thieno[3,4-*d*]imidazol-4-yl)-*N*-(4-(2-(pyridin-2-ylmethylene)hydrazine-1-carbothioamido)butyl)pentanamide (BioFTSC2). A solution of Biotin-NHS (0.20 g, 0.58 mmol) in abs. DMF (3 mL) was added to a suspension of **4b** (0.19 g, 0.58 mmol) and Et_3N (0.24 mL, 1.74 mmol) in abs. DMF (3 mL) and the reaction mixture was stirred overnight. Water (25 mL) was added and the white precipitate was filtered off, washed with water and dried in *vacuo*. The product was recrystallized from water. Yield: 0.23 g (80 %). Anal. Calcd for $C_{21}H_{31}N_7O_2S_2{\cdot}0.5H_2O$ (M_r = 486.66 g/mol): C, 51.83; H, 6.63; N, 20.15; S, 13.18. Found: C, 51.55; H, 6.68; N, 20.14; S, 13.00. ESI-MS in methanol (positive): *m*/*z* 478, $[M+H]^+$. ^{1}H NMR (500.10 MHz, DMSO-d_6): δ 11.65 (s, 1H, (C=N)NH), 8.69 (t, ^3J = 6 Hz, 1H, (C=S)N*H*CH_2), 8.59–8.56 (m, 1H, H_{py}), 8.28 (d, ^3J = 8 Hz, 1H, H_{py}), 8.10 (s, 1H, HC=N), 7.88–7.83 (ddd, ^3J = 8 Hz, ^3J = 8 Hz, ^4J = 2 Hz, 1H, H_{py}), 7.78 (t, ^3J = 6 Hz, 1H,

*H*N(C=O)CH_2), 7.41–7.37 (ddd, ^3J = 7 Hz, ^3J = 5 Hz, ^4J = 1 Hz, 1H, H_{py}), 6.41 (s, 1H, *H*N(C=O)NH), 6.35 (s, 1H, HN(C=O)N*H*), 4.33–4.28 (m, 1H, *H*C-CH), 4.15–4.11 (m, 1H, HC-C*H*), 3.61–3.55 (m, 2H, (C=S)NHCH_2), 3.13–3.05 (m, 3H, CH_2NH(C=O) and CHS), 2.82 (dd, ^2J = 13 Hz, ^3J = 5 Hz, 1H, SCH_2), 2.58 (d, ^2J = 12 Hz, 1H, SCH_2), 2.06 (t, ^3J = 7 Hz, 2H, (C=O)CH_2), 1.62–1.23 (m, 10H, (C=O)CH_2CH_2CH_2CH_2 and HNCH_2CH_2C$H_2$$CH_2$NH) ppm. ^{13}C NMR (125.81 MHz, DMSO-d_6): δ 177.6 (C=S), 172.3 (CH_2NH(*C*=O)), 163.2 (HN(C=O)NH), 153.5 ($C_{q,\ py}$), 149.5 (C_{py}), 142.1 (HC=N), 137.4 (C_{py}), 124.6 (C_{py}), 120.9 (C_{py}), 61.5 (H*C*-CH), 59.7 (HC-*C*H), 55.9 (CHS), 43.8 ((C=S)NH*C*H_2), 40.1 (SCH_2), 38.7 (*C*H_2NH(C=O)), 35.7 ((C=O)*C*H_2), 28.7, 28.5 and 25.8 ((C=O)CH_2*C*H_2*C*H_2*C*H_2), 27.2 and 26.9 ((C=S)NHCH_2*C*H_2*C*$H_2$$CH_2$NH).

(*E*)-*N*-(4-(2-((3-aminopyridin-2-yl)methylene)hydrazine-1-carbothioamido)butyl)-5-(2-oxohexahydro-1*H*-thieno[3,4-*d*]imidazol-4-yl)pentanamide (BioTriapine). Biotin-NHS (0.30 g, 0.88 mmol) was added portionwise to a suspension of **4c** (0.30 g, 0.88 mmol) and Et_3N (0.37 mL, 2.64 mmol) in 9 mL abs. DMF and the reaction mixture was stirred overnight. Water (46 mL) was added and the pale yellow precipitate was filtered off, washed with water and dried in *vacuo*. Yield: 0.37 g (84 %). Anal. Calcd for $C_{21}H_{32}N_8O_2S_2 \cdot H_2O$ (M_r = 510.68 g/mol): C, 49.39; H, 6.71; N, 21.94; S, 12.56. Found: C, 49.61; H, 6.64; N, 21.51; S, 12.53. ESI-MS in methanol (positive): *m*/*z* 493, $[M+H]^+$. ^{1}H NMR (500.10 MHz, DMSO-d_6): δ 11.29 (s, 1H, (C=N)NH), 8.37 (t, ^3J = 5 Hz, 1H, (C=S)NHCH_2), 8.34 (s, 1H, HC=N), 7.85 (dd, ^2J = 4 Hz, ^3J = 1 Hz, 1H, H_{py}), 7.78 (t, ^3J = 6 Hz, 1H, NHC=O), 7.17 (dd, ^2J = 7 Hz, ^3J = 1 Hz, 1H, H_{py}), 7.09 (dd, ^2J = 8 Hz, ^3J = 4 Hz, 1H, H_{py}), 6.45 (s, 2H, NH_2), 6.42 (s, 1H, *H*N(C=O)NH), 6.35 (s, 1H, HN(C=O)N*H*),

4.33–4.28 (m, 1H, *H*C-CH), 4.15–4.11 (m, 1H, HC-C*H*), 3.60–3.53 (m, 2H, (C=S)NHCH_2), 3.12–3.04 (m, 3H, CH_2NHC=O and CHS), 2.82 (dd, ^2J = 12 Hz, ^3J = 5 Hz, 1H, SCH_2), 2.58 (d, ^2J = 12 Hz, 1H, SCH_2), 2.06 (t, ^3J = 7 Hz, 2H, NH(C=O)CH_2), 1.66–1.24 (m, 10H, (C=O)CH_2CH_2CH_2CH_2 and HNCH_2CH_2CH_2CH_2NH) ppm. ^{13}C NMR (125.81 MHz, DMSO-d_6): δ 176.8 (C=S), 172.3 (NH(*C*=O)CH_2), 163.2 (HN(C=O)NH), 148.4 (HC=N), 144.4 ($C_{q,\ py}$), 137.3 (C_{py}), 133.1 ($C_{q,\ py}$), 125.0 (C_{py}), 123.2 (C_{py}), 61.5 (H*C*-CH), 59.7 (HC-*C*H), 55.9 (CHS), 44.0 ((C=S)HN*C*H_2), 40.1 (SCH_2), 38.8 (*C*H_2NHC=O), 35.7 (NH(C=O)*C*H_2), 28.7, 28.5 and 25.8 ((C=O)CH_2*C*H_2*C*H_2*C*H_2), 27.2 and 27.1 ((C=S)HNCH_2*C*H_2*C*H_2CH_2NH).

(*E*)-*N*-(4-(2-((3-aminopyridin-2-yl)methylene)hydrazine-1-carbothioamido)butyl)-5-(2-oxohexahydro-1*H*-thieno[3,4-*d*]imidazol-4-yl)pentanamide-*N,N,S*-dichloridocopper(II), [Cu(BioTriapine)Cl_2]·H_2O. To **BioTriapine** (50 mg, 0.102 mmol) dissolved in hot methanol (5 mL), copper(II)chloride dihydrate (17 mg, 0.102 mmol) in methanol (0.5 mL) was added dropwise, and the reaction mixture was stirred for 2 h at room temperature. The green precipitate was filtered off, washed with methanol and diethyl ether, and dried in *vacuo*. Yield: 53 mg (81 %). Anal. Calcd for $CuC_{21}H_{32}N_8O_2S_2Cl_2·H_2O$ (M_r = 645,13 g/mol): C, 39.10; H, 5.31; N, 17.37; S, 9.94. Found: C, 39.37; H, 5.28; N, 17.03; S, 9.97. ESI-MS in methanol (positive): *m*/*z* 554, $[M-2Cl-H]^+$ ESI-MS in methanol (negative): *m*/*z* 588, $[M-2H-Cl]^-$; *m*/*z* 624, $[M-H]^-$.

[Bis(*E*)-*N*-(4-(2-((3-aminopyridin-2-yl)methylene)hydrazine-1-carbothioamido)butyl)-5-(2-oxohexahydro-1*H*-thieno[3,4-*d*]imidazol-4-yl)pentanamide-*N,N,S*-iron(III)] nitrate, [Fe(BioTriapine)$_2$]NO_3·3.5H_2O. To

BioTriapine (80 mg, 0.162 mmol) and *N*-methylmorpholine (18 µL, 0.161 mmol) in methanol (3.5 mL) iron(III) nitrate nonahydrate (33 mg, 0.81 mmol) in methanol (0.5 mL) was added dropwise and the reaction mixture was stirred for 2 h at room temperature. After addition of ethyl acetate (5 mL), the dark brown precipitate was filtered off, washed with ethyl acetate and dried in *vacuo*. The crude product was taken up in methanol and purification by preparative RP-HPLC using a Waters XBridge C18 column on an Agilent 1200 Series system yielding a brown solid (Milli-Q water and acetonitrile were used as eluents). Yield: 22 mg (42 %). Anal. Calcd for $FeC_{42}H_{62}N_{17}O_7S_4 \cdot 3.5H_2O$ (M_r = 1164,21 g/mol): C, 43.33; H, 5.97; N, 20.45; S, 11.02. Found: C, 43.66; H, 5.77; N, 20.05; S, 10.96. ESI-MS in methanol (positive): *m*/*z* 1038, $[M]^+$.

Electrochemistry

Cyclic voltammograms were measured in a three-electrode cell using a 2.0-mm-diameter glassy carbon working electrode, a platinum auxiliary electrode and an Ag/AgCl reference electrode containing 3.0 M NaCl. Measurements were performed at room temperature using EG & G PARC 273A potentiostat/galvanostat. Deaeration of solutions was accomplished by passing a stream of argon through the solution for 5 min prior to measurement and then maintaining blanket atmosphere of argon over the solution during measurement. The potentials were measured in DMF/phosphate-buffered saline (PBS) pH 7.4 (2:1 v/v) containing 0.10 M [*n*-Bu_4N][BF_4] and are quoted relative to the normal hydrogen electrode (NHE). To convert the obtained potentials (vs. Ag/AgCl) to values vs. NHE, +0.209 V was added to the measured results.

Spectrophotometric titrations

A Hewlett Packard 8452A diode array spectrophotometer was used to record the UV-Vis spectra in the interval 200–800 nm. The path length was 1 cm. Proton dissociation constants (pK_a) of the ligands, the copper(II) mono complexes and the individual spectra of the species in the various protonation states were calculated by the computer program PSEQUAD[54]. Spectrophotometric titrations were performed on samples containing the ligands or complexes at 25-75 μM concentration by a KOH solution in the presence of 0.1 M KCl at 25.0 ± 0.1 °C in the pH range from 2.0 to 11.9. An Orion 710A pH-meter equipped with a Metrohm combined electrode (type 6.0234.100) and a Metrohm 665 Dosimat burette were used for the pH-metric titrations. The electrode system was calibrated to the pH = log[H^+] scale by means of blank titrations (HCl vs. KOH) according to the method suggested by Irving *et al.*[55]. The average water ionization constant (pK_w) is 13.76 ± 0.05 in water. Argon was also passed over the solutions during the titrations.

The conditional stability constants (*β*') of the copper(II) complexes were calculated at pH 5.90 based on the spectral changes *via* the displacement reaction with EDTA in the presence 50 mM 2-(*N*-morpholino)ethanesulfonic acid (MES) and 0.1 M KCl. In the competition experiments the samples contained 25 μM copper(II), 25 μM ligand and the concentration of EDTA was varied in the range from 0 to 100 μM. The conditional stability constants of the metal complexes (*β'* (CuL)) and the individual spectra of the species were calculated by the computer program PSEQUAD[54]. The overall stability constants of the $[CuL]^+$ complexes (*β*) were calculated from the conditional stability constants: $\beta\ [CuL]^+ = \beta'\ [CuL]^+ \times \alpha_H$, where $\alpha_H = 1 + [H^+]/K_a\ (HL) + [H^+]^2 / (K_a\ (HL) \times K_a\ (H_2L^+))$; $[H^+] = 10^{-5.90}$ M. The overall stability constants of the

protonated $[CuLH]^{2+}$ and the mixed hydroxido [CuL(OH)] complexes were calculated as follows: log β $[CuLH]^{2+}$ = log β $[CuL]^{+}$ + pK_a $[CuLH]^{2+}$. Log β [CuL(OH)] = log β $[CuL]^{+}$ – pK_a $[CuL]^{+}$.

Spectrophotometric reduction kinetic measurements

The redox reactions of the metal complexes (with concentrations of 50 µM in PBS pH 7.4) with 20 equivalents AA, GSH and DTT were studied on a Perkin Elmer lambda 35 spectrophotometer with a PTP 6 (Peltier Temperature Programmer) and Julabo AWC 100 recirculating cooler at 25°C. Spectra were recorded before and after addition of the reducing agents and changes were followed for 20 min.

Cell culture

The following human cancer cell lines were used in this study: The colorectal carcinoma-derived cell lines HCT116 and CT26 as well as the breast cancer cell lines SKBR-3, MCF-7, and MDA-MB-231. All cell lines were grown in Dulbecco's Modified Eagle's medium (DMEM) supplemented with 10% fetal bovine serum (FBS) at 37°C and 5% CO_2, with the exception of HCT116, which were grown in McCoy’s medium supplemented with 2 mM glutamine and 10%FBS and CT26 grown in DMEM/F-12 supplemented with 10% FCS. In addition, the non-malignant fibroblasts HLF (in RPMI1640 with 10% FCS) and keratinocytes HACAT (in DMEM with 10% FCS) were tested. All cells were purchased from ATCC and regularly checked for *Mycoplasma* contamination.

Cellular biotin uptake

Cells (5 x 10^5 cells/mL in 1 mL growth medium per well) were seeded in 6-well plates and allowed to attach for 24 h. Then, growth medium was replaced with 2 mL serum-free medium (RPMI 1640) per well. On the following day, the cells were treated with 25 mM FITC-labeled biotin. After 6 h incubation, cells were washed twice with phosphate-buffered saline (PBS) and collected by trypsinisation. The suspension was centrifuged for 5 min at 1200 rpm at 4°C and the supernatant discarded. For flow cytometry, the cells were re-suspended in PBS containing 78.1 mM Na_2PO_4 x $2H_2O$, 14.7 mM KH_2PO_4, 26.8 mM KCl and 1.37 M NaCl, followed by analyses of the intracellular fluorescence levels (FITC) measured by LSRFortessa flow cytometer (BD Biosciences, New Jersey, USA) and further analyzed using Flowing Software (University of Turku, Finland) to quantify the intracellular fluorescent units.

Cell viability assay

To determine cell viability, depending on the cell line, 2-5 x 10^4 cells/mL were seeded in 96-well plates (100 µL/well) and allowed to recover for 24 h. Then, cells were exposed to the drugs for the indicated concentrations for 72 h. Anticancer activity was measured by the 3-(4,5-dimethylthiazol-2-yl)-2,5-diphenyltetrazolium bromide (MTT)-based vitality assay following the manufacturer's recommendations (EZ4U, Biomedica, Vienna, Austria). Cell viability was calculated using the Graph Pad Prism software (using a point-to-point function) and was expressed as IC_{50} values calculated from full dose-response curves (drug concentrations inducing a 50% reduction of cell number in comparison to untreated control cells cultured in parallel).

ICP-MS

To determine cellular accumulation of the Cu-containing drugs, cells were incubated with 25 µM and 50 µM of the copper complexes and copper(II) chloride for 4 h at 37 °C, washed twice with PBS and then lysed in 500 µL of tetramethylammonium hydroxide at room temperature for 5 min. The obtained lysates were dissolved in 25 mL 0.6 M HNO_3. Copper concentrations were determined using an Agilent ICP-MS 7900 (Agilent Technologies, Santa Clara, CA).

Long-term cell viability (Clonogenic assay)

To examine long time cell viability, 1 x 10^3 cells/mL of HCT116 and 2 x 10^3 cells/mL of MCF-7 were seeded in 24-well plates (500 µL/well) and allowed to recover for 24 h. Then, cells were exposed to the drugs (100 µL/well) for the indicated concentrations for 9 days. After incubation, the medium was removed and the wells dried overnight. The following day, the cells were washed once with 300 µL PBS per well and were then fixed with 300 µL methanol per well. Afterwards, cells were stained with crystal violet, washed with water and dried overnight. Grey scaled pictures of the wells were made by scans using a Typhoon machine. The anticancer activity was measured by analyzing these pictures with ImageJ.

Animals

Eight- to twelve-week-old Balb/c mice were purchased from Harlan (Italy) and were housed under standard conditions with a 12 h light-dark cycle at the animal research

facility with *ad libitum* access to food and water. The experiments were performed according to the Federation of Laboratory Animal Science Association guidelines for the use of experimental animals and were approved by the Ethics Committee for the Care and Use of Laboratory Animals at the Medical University Vienna and the Ministry of Science and Research, Austria (BMWF-66.009/0084-II/3b/2013). With regard to the execution of our animal experiments, we followed the ARRIVE guidelines.

CT26 experiment in vivo

The anticancer activity of BioTriapine was investigated in vivo using murine colon cancer cells (CT-26). For this, 5 x 10^5 cells in 50 µL were injected subcutaneously into the right flank of the mice. When tumor nodules were palpable, animals were treated orally with **BioTriapine** (25 mg/kg in 10% DMSO) on 5 subsequent days for two cycles. Body weight and tumor growth were measured every second day using a micro-caliper. Tumor size was assessed by caliper measurement and tumor volume calculated using the formula: (length x width^2)/2.

Generation of superoxide radicals and H_2O_2 formation assays

To examine cell-free production of H_2O_2, the PerOXO-quant assay (Pierce, Rockford, IL, USA) was used according to the manufacturer's recommendations and as described previously [33]. For investigation of the cell-free production of superoxide radicals of the complexes, the reduction of NBT was analyzed as described in our previous publication[33].

Abbreviations: AA: ascorbic acid; APTSC: 3-aminopyridine-2-carboxyaldehyde-^{4}N,^{4}N-dimethylthiosemicarbazone; BioFTSC1: (*E*)-5-(2-oxohexahydro-1*H*-thieno[3,4-*d*]imidazol-4-yl)-*N*-(2-(2-(pyridin-2-ylmethylene)hydrazine-1-carbothioamido)ethyl)pentanamide; BioFTSC2: (*E*)-5-(2-oxohexahydro-1*H*-thieno[3,4-*d*]imidazol-4-yl)-*N*-(4-(2-(pyridin-2-ylmethylene)hydrazine-1-carbothioamido)butyl)pentanamide; BioTriapine: (*E*)-*N*-(4-(2-((3-aminopyridin-2-yl)methylene)hydrazine-1-carbothioamido)butyl)-5-(2-oxohexahydro-1*H*-thieno[3,4-*d*]imidazol-4-yl)pentanamide; DMF: dimethylformamide; DMSO: dimethyl sulfoxide; DTT: dithiothreitol; ESI: electrospray ionization; FTSC: 2-formylpyridine thiosemicarbazone; GSH: glutathione; NBT: nitro blue tetrazolium; NAC: *N*-acetylcysteine; NHE: normal hydrogen electrode; PBS: phosphate-buffered saline; RR: ribonucleotide reductase; SMVT: sodium-dependent multivitamin transporter.

Acknowledgements

This work was supported by the Mahlke geb. Obermann-Stiftung of the University of Vienna FA526009 (to B. Keppler) and the National Research, Development and Innovation Office-NKFI through project FK 124240 (to E. Enyedy). Lukas Uhlik was financed by the Fellinger Krebsforschungsverein. Many thanks to Gerhard Zeitlinger for the devoted animal care.

References:

[1] R.W. Brockman, J.R. Thomson, M.J. Bell, H.E. Skipper, Cancer Res, vol. 16, 1956, pp. 167-170.

[2] P. Heffeter, V.F. Pape, E.A. Enyedy, B.K. Keppler, G. Szakas, C.R. Kowol, Antioxid Redox Signal, 2018.

[3] M. Kolberg, K.R. Strand, P. Graff, K. Kristoffer Andersson, Biochim Biophys Acta, vol. 1699, 2004, pp. 1-34.

[4] M.-C. Liu, T.-S. Lin, A.C. Sartorelli, Prog Med Chem, vol. 32, 1995, pp. 1-35.

[5] K. Agrawal, A. Sartorelli, Prog Med Chem, vol. 15, 1978, pp. 321-356.

[6] É.A. Enyedy, É. Zsigó, N.V. Nagy, C.R. Kowol, A. Roller, B.K. Keppler, T. Kiss, Eur J Inorg Chem, vol. 2012, 2012, pp. 4036-4047.

[7] É.A. Enyedy, N.V. Nagy, É. Zsigó, C.R. Kowol, V.B. Arion, B.K. Keppler, T. Kiss, Eur J Inorg Chem, vol. 2010, 2010, pp. 1717-1728.

[8] J. Murren, M. Modiano, C. Clairmont, P. Lambert, N. Savaraj, T. Doyle, M. Sznol, Clin Cancer Res, vol. 9, 2003, pp. 4092-4100.

[9] S. Attia, J. Kolesar, M.R. Mahoney, H.C. Pitot, D. Laheru, J. Heun, W. Huang, J. Eickhoff, C. Erlichman, K.D. Holen, Invest New Drugs, vol. 26, 2008, pp. 369-379.

[10] S. Wadler, D. Makower, C. Clairmont, P. Lambert, K. Fehn, M. Sznol, J Clin Oncol, vol. 22, 2004, pp. 1553-1563.

[11] C. Nutting, C. Van Herpen, A. Miah, S. Bhide, J.-P. Machiels, J. Buter, C. Kelly, D. De Raucourt, K. Harrington, Ann Oncol, vol. 20, 2009, pp. 1275-1279.

[12] B. Ma, B.C. Goh, E.H. Tan, K.C. Lam, R. Soo, S.S. Leong, L.Z. Wang, F. Mo, A.T.C. Chan, B. Zee, T. Mok, Invest New Drugs, vol. 26, 2008, pp. 169-173.

[13] J.J. Knox, S.J. Hotte, C. Kollmannsberger, E. Winquist, B. Fisher, E.A. Eisenhauer, Invest New Drugs, vol. 25, 2007, pp. 471-477.

[14] K. Pelivan, L. Frensemeier, U. Karst, G. Koellensperger, B. Bielec, S. Hager, P. Heffeter, B.K. Keppler, C.R. Kowol, Analyst, vol. 142, The Royal Society of Chemistry, 2017, pp. 3165-3176.

[15] K. Pelivan, W. Miklos, S. van Schoonhoven, G. Koellensperger, L. Gille, W. Berger, P. Heffeter, C.R. Kowol, B.K. Keppler, J Inorg Biochem, vol. 160, 2016, pp. 61-69.

[16] L. Feun, M. Modiano, K. Lee, J. Mao, A. Marini, N. Savaraj, P. Plezia, B. Almassian, E. Colacino, J. Fischer, Cancer Chemother Pharmacol, vol. 50, 2002, pp. 223-229.

[17] M. Whitnall, J. Howard, P. Ponka, D.R. Richardson, Proc Natl Acad Sci, vol. 103, 2006, pp. 14901-14906.

[18] Z. Kovacevic, S. Chikhani, D.B. Lovejoy, D.R. Richardson, Mol Pharmacol, 2011, pp. mol. 111.073627.

[19] W. Xia, P.S. Low, J Med Chem, vol. 53, 2010, pp. 6811-6824.

[20] P.S. Low, W.A. Henne, D.D. Doorneweerd, Acc Chem Res, vol. 41, 2007, pp. 120-129.

[21] G. Tripodo, D. Mandracchia, S. Collina, M. Rui, D. Rossi, Med Chem, vol. 8, 2014, pp. 1-4.

[22] I. Niculescu-Duvaz, Curr Opin Investig Drugs, vol. 3, 2002, pp. 1527-1532.

[23] E.A. Akam, E. Tomat, Bioconjugate Chem, vol. 27, 2016, pp. 1807-1812.

[24] S. Maiti, N. Park, J.H. Han, H.M. Jeon, J.H. Lee, S. Bhuniya, C. Kang, J.S. Kim, J Am Chem Soc, vol. 135, American Chemical Society, 2013, pp. 4567-4572.

[25] J.G. Vineberg, E.S. Zuniga, A. Kamath, Y.-J. Chen, J.D. Seitz, I. Ojima, J Med Chem, vol. 57, American Chemical Society, 2014, pp. 5777-5791.

[26] K. Mitra, A. Shettar, P. Kondaiah, A.R. Chakravarty, Inorg Chem, vol. 55, American Chemical Society, 2016, pp. 5612-5622.

[27] J. Zempleni, S.S. Wijeratne, Y.I. Hassan, Biofactors, vol. 35, 2009, pp. 36-46.

[28] J. Zempleni, Annu Rev Nutr, vol. 25, 2005, pp. 175-196.

[29] R.J. McMahon, Annu Rev Nutr, vol. 22, 2002, pp. 221-239.

[30] S. Chen, X. Zhao, J. Chen, J. Chen, L. Kuznetsova, S.S. Wong, I. Ojima, Bioconjugate Chem, vol. 21, American Chemical Society, 2010, pp. 979-987.

[31] B. Fischer, K. Kryeziu, S. Kallus, P. Heffeter, W. Berger, C.R. Kowol, B.K. Keppler, RSC Adv, vol. 6, The Royal Society of Chemistry, 2016, pp. 55848-55859.

[32] P.J. Jansson, P.C. Sharpe, P.V. Bernhardt, D.R. Richardson, J Med Chem, vol. 53, American Chemical Society, 2010, pp. 5759-5769.

[33] C.R. Kowol, P. Heffeter, W. Miklos, L. Gille, R. Trondl, L. Cappellacci, W. Berger, B.K. Keppler, J Biol Inorg Chem, vol. 17, 2012, pp. 409-423.

[34] C.R. Kowol, R. Trondl, P. Heffeter, V.B. Arion, M.A. Jakupec, A. Roller, M. Galanski, W. Berger, B.K. Keppler, J Med Chem, vol. 52, American Chemical Society, 2009, pp. 5032-5043.

[35] W.X. Ren, J. Han, S. Uhm, Y.J. Jang, C. Kang, J.H. Kim, J.S. Kim, Chem Commun, vol. 51, 2015, pp. 10403-10418.

[36] Y. Uchida, K. Ito, S. Ohtsuki, Y. Kubo, T. Suzuki, T. Terasaki, J Neurochem, vol. 134, 2015, pp. 97-112.

[37] É.A. Enyedy, M.F. Primik, C.R. Kowol, V.B. Arion, T. Kiss, B.K. Keppler, Dalton Trans, vol. 40, 2011, pp. 5895-5905.

[38] W.E. Antholine, J.M. Knight, D.H. Petering, Inorg Chem, vol. 16, 1977, pp. 569-574.

[39] J. Felcman, J.F. Da Silva, Talanta, vol. 30, 1983, pp. 565-570.

[40] T. Jakusch, É.A. Enyedy, K. Kozma, Z. Paár, A. Bényei, T. Kiss, Inorg Chim Acta, vol. 420, 2014, pp. 92-102.

[41] A. Seo, J.L. Jackson, J.V. Schuster, D. Vardar-Ulu, Anal Bioanal Chem, vol. 405, 2013, pp. 6379-6384.

[42] J. García-Tojal, R. Gil-García, V.I. Fouz, G. Madariaga, L. Lezama, M.S. Galletero, J. Borrás, F.I. Nollmann, C. García-Girón, R. Alcaraz, J Inorg Biochem, vol. 180, 2018, pp. 69-79.

[43] F.Q. Schafer, G.R. Buettner, Free Radical Biol Med, vol. 30, 2001, pp. 1191-1212.

[44] W.W. Cleland, Biochemistry, vol. 3, 1964, pp. 480-482.

[45] U. Jungwirth, C.R. Kowol, B.K. Keppler, C.G. Hartinger, W. Berger, P. Heffeter, Antioxid Redox Signal, vol. 15, 2011, pp. 1085-1127.

[46] R. Kumar, J. Han, H.-J. Lim, W.X. Ren, J.-Y. Lim, J.-H. Kim, J.S. Kim, J Am Chem Soc, vol. 136, 2014, pp. 17836-17843.

[47] N. Muhammad, N. Sadia, C. Zhu, C. Luo, Z. Guo, X. Wang, Chem Commun, vol. 53, The Royal Society of Chemistry, 2017, pp. 9971-9974.

[48] M.V. Babak, D. Plażuk, S.M. Meier, H.J. Arabshahi, J. Reynisson, B. Rychlik, A. Błauż, K. Szulc, M. Hanif, S. Strobl, Chem Eur J, vol. 21, 2015, pp. 5110-5117.

[49] W. Hu, L. Fang, W. Hua, S. Gou, J Inorg Biochem, vol. 175, 2017, pp. 47-57.

[50] D.R. Richardson, D.S. Kalinowski, V. Richardson, P.C. Sharpe, D.B. Lovejoy, M. Islam, P.V. Bernhardt, J Med Chem, vol. 52, 2009, pp. 1459-1470.

[51] C. Schmuck, J. Dudaczek, Eur J Org Chem, vol. 2007, 2007, pp. 3326-3330.

[52] P.D. Bonnitcha, S.R. Bayly, M. Theobald, H.M. Betts, J.S. Lewis, J.R. Dilworth, J Inorg Biochem, vol. 104, 2010, pp. 126-135.

[53] X. Jiang, M. Ahmed, Z. Deng, R. Narain, Bioconjugate Chem, vol. 20, 2009, pp. 994-1001.

[54] L. Zékány, I. Nagypál, Computational Methods for the Determination of Formation Constants, Springer, 1985, pp. 291-353.

[55] H. Irving, M. Miles, L. Pettit, Anal Chim Acta, vol. 38, 1967, pp. 475-488.